MONTHLY NOTICES

OF THE

ROYAL ASTRONOMICAL SOCIETY

Vol. 106 No. 2

## MEETING OF 1946 MARCH 8

Professor H. H. Plaskett, President, in the Chair

The election by the Council of the following Fellows was duly confirmed:—

Gordon Atwater, American Museum of Natural History, Central Park West at 79th Street, New York, U.S.A.;
Frederick Edward Brasch, Library of Congress, Washington, U.S.A.;
George B. Burnside, Fairhill, Dullatur, Dumbartonshire;
James Henry John Burtt, 6 Elmbourne Road, London, S.W. 17;
Dorothy B. G. Hawkins, M.A., Hacks Wood, Walton-in-Gordano, near Clevedon, Somerset;
James Samuel Houston, B.E., A.M.I.C.E., G.P.O. Box 29 F, Hobart, Tasmania, Australia; and
William Henry Julian, B.Sc., 8 Trelawny Road, St. Austell, Cornwall.

The following candidates were proposed for election as Fellows of the Society, the names of the proposers from personal knowledge being appended:—

Hermann Bondi, Fellow of Trinity College, Cambridge (proposed by F. Hoyle);
Norman Frank Henry Knight, 72 Chadacre Road, Stoneleigh, Epsom, Surrey (proposed by W. M. Lindley); and
Charles Arthur Padgham, 6 Manor Cottages, Lamberhurst, Tunbridge Wells, Kent (proposed by A. D. Thackeray).

Forty-nine presents were announced as having been received since the last meeting, including:—

British Association, *Mathematical Tables*, Vols. I and IX (presented by the British Association Tables Committee).

# ON THE INCLINATION OF THE NORMAL AXES OF SUNSPOTS

*M. G. J. Minnaert, Assoc. R.A.S.*

(Received 1946 January 24)

*Summary*

By a simple method the inclination of the axes is derived from the asymmetry in the observed total area, independently of any assumptions concerning the rate of foreshortening. The inclination found amounts to 0°·44 for all spots, 4°·3 and 6°·8 for long-lived spots of 13 and 14 days' duration, 7°·6 for recurrent spots.

---

The asymmetry, found by Mrs. A. S. D. Maunder * in the distribution of sunspots over the solar disk, may be reduced to two principal statements:

(1) more spots *are formed* on the E. than on the W. hemisphere;
(2) at any moment, more spots *occur* on the E. than on the W. hemisphere.

The first phenomenon has been explained already long ago by Schuster, and has been analysed further by Gleissberg, Waldmeier, Archenhold and myself. For the second phenomenon Mrs. Maunder suggested the explanation that the normal axes of the spots are slightly inclined to the solar radius, sloping downward from west to east, and that thereby their visibility is increased on one hemisphere and diminished on the other.

By a simple calculation, Gleissberg † determined the inclination which is necessary in order to produce the observed asymmetry. He starts from the assumption, that if a spot is directed along a solar radius, its area $S$ will be observed as $S \cos \lambda$, $\lambda$ being the angle between the meridian of the spot and the central meridian of the Sun. If the spot is inclined at an angle $i$ to the solar radius, we will observe its area as $S \cos (\lambda - i)$ on the E. hemisphere and as $S \cos (\lambda + i)$ on the W. hemisphere. We simply have to select an inclination $i$ for which the ratio $\dfrac{\cos (\lambda - i)}{\cos (\lambda + i)}$ corresponds to the observed asymmetry. Taking together all the spots treated by Mrs. Maunder, Gleissberg found that an angle of 0°·6 is sufficient to explain the observations.

This computation is entirely based on the assumption that the spots are foreshortened by perspective in the ratio $\cos \lambda$. However, a recent investigation by Archenhold ‡ shows conclusively that this is not the case: in addition to the geometrical foreshortening, there is also a "physical foreshortening". Fortunately we may dismiss any theoretical presupposition concerning the ratio in which the areas are reduced when they are not perpendicular to the line of sight. The axis of a spot at a distance $\lambda$ from the central

* *M.N.*, 67, 451, 1907.
† *Publ. Istanbul Univ. Obs.*, No. 12, 1940.
‡ *M.N.*, 100, 645, 1940.

meridian, inclined at an angle $i$ to the radius, will form an angle $\lambda - i$ with our line of sight on the E. hemisphere, $\lambda + i$ on the W. hemisphere. If we observe a greater area for the spots near meridian $-\lambda$ than $+\lambda$, we will have to determine the neighbouring longitudes $\lambda + i$ on the E. side and $\lambda - i$ on the W. side for which the spot areas are found equal. The angle $i$ thus determined is the inclination of the spot axes.

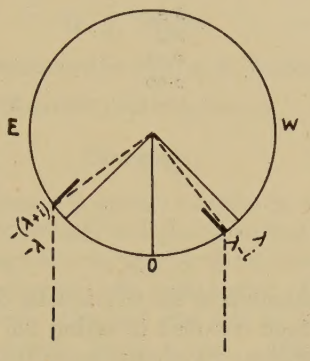


This method is not entirely unobjectionable. It is not certain that the apparent area of a spot is only a function of its inclination to the line of sight; it could be that the inclination of the solar surface plays also a rôle. But still our simple assumption is the only convenient starting-point, and so we will make use of it just as Gleissberg did. In any case we have minimized the objections by applying the empirical foreshortening. The calculation proceeds by the following steps:—

1. Mrs. Maunder has divided the solar surface into 14 lunes, corresponding each to about 13° of longitude. For each of these she gives the total observed area of the spots, multiplied by $1/\cos\lambda$ to correct for geometrical foreshortening. We begin by reducing back these numbers to the directly observed areas $S$.
2. We plot the mean area of the spots for each lune against the longitude $\lambda$, and we determine at what rate it decreases per degree. Over a great part of the solar disk, the gradient $dS/d\lambda$ happens to be nearly constant and can best be determined numerically; in the central part it has to be deduced graphically from the slope of our plot.
3. We compare the spot areas $S$, $S'$ of two lunes, symmetrically placed with respect to the central meridian, and we take the mean value of $dS/d\lambda$. We now determine $\Delta\lambda$ so that

$$\frac{dS}{d\lambda}\Delta\lambda = \frac{S - S'}{2}.$$

The inclination of the spot axes $i$ is equal to $\Delta\lambda = \frac{1}{2}(S - S')/(dS/d\lambda)$.

This computation was made:

(*a*) for the totality of the sunspots (Mrs. Maunder, Table III);
(*b*) for the long-lived spots, observed during 13 or 14 consecutive days on the visible disk (her Table X);
(*c*) for the recurrent spots, of which at least three passages over the disk were observed, the statistics relating only to the intermediate passage (her Table XV).

In all these cases, effects of "phase" or varying rates of growth of the spots are excluded. The values of the gradient were of course determined separately for each of the computations (*a*), (*b*), (*c*). The method will be sufficiently illustrated by the following table, relating to section (*a*):—

| Mean | Area | Asymmetry | Gradient | Inclination |
|---|---|---|---|---|
| | $S$ | $S-S'$ | $dS/d\lambda$ | $i$ |
| ° | | | | ° |
| −85 | 5·2 | 1·0 | 3·2 | *0·16* |
| −72·5 | 51·1 | 2·4 | 3·6 | 0·33 |
| −59·5 | 102·4 | 2·5 | 3·7 | 0·34 |
| −46 | 152·1 | 5·5 | 3·3 | 0·83 |
| −33 | 191·2 | 2·4 | 2·7 | 0·44 |
| −20 | 219·35 | 0·90 | 1·67 | 0·27 |
| − 6·5 | 233·71 | 0·66 | 0·80 | 0·41 |
| + 6·5 | 233·05 | | | Mean 0·44 |
| +20 | 218·45 | | | |
| +33 | 188·9 | | | |
| +46 | 146·6 | | | |
| +59·5 | 99·9 | | | |
| +72·5 | 48·7 | | | |
| +85 | 4·2 | | | |

All areas are expressed in thousandths of the visible solar disk, all angles in degrees. The first and last lunes have not been included in taking the mean, because observations in these lunes are certainly less reliable; the circumstance that spots are not being registered continuously but with intervals of one day has a great influence on the counts for these lunes.

The final results of our computations may be summarised as follows:—

(*a*) all spots . . . . . $i=0{\cdot}44°$
(*b*) long-lived spots of a duration of 13 days at least . $i=4{\cdot}3$
" " " " 14 " " . . $i=6{\cdot}8$
(*c*) recurrent spots . . . . . $i=7{\cdot}6$

It will be seen that the inclinations of spot axes for section (*a*) are even smaller than those deduced by Gleissberg. This was to be expected, since the empirical foreshortening is more pronounced than the function cos $\lambda$, used by him.

Moreover, we find that long-lived spots show a much greater inclination, this inclination increasing together with their duration. This result is in satisfactory agreement with the current explanation for the origin of the inclination: the angular velocity of rotation of the solar layers increases with the latitude, so that a radial vortex will gradually slope downward. The longer a spot exists, the more pronounced will be this effect of the velocity differences.

*Sterrewacht Sonnenborgh,*
*Utrecht:*
1946 *January* 17.

# STRUCTURE OF SUNSPOTS

*G. J. Odgers*

(Communicated by R. v. d. R. Woolley)

(Received 1946 February 7)

*Summary*

The possibility that a sunspot is merely a region in which the product of the absorption coefficient and the density is higher than that of the disk is examined. The equations of radiative equilibrium appropriate to this case are derived and are found to admit of an exact solution. An examination of this solution shows that the observed contrast between spot and disk can be accounted for by merely postulating an increase of density inside a spot. Other features of spots are also explained in this way, namely the penumbra and the so-called bright ring.

---

1. In this paper certain characteristics of sunspots are given a simple explanation in terms of the supposition that a spot is merely a region wherein the absorption coefficient (strictly speaking the product of the mass absorption coefficient and the density) differs from that of the disk.

Two very striking features of spots have long been known. The study of the total amount of light and of the relative intensities of lines in sunspot and solar spectra shows that spots are considerably cooler than the photosphere.* The former study also shows that the light flux across the umbra bears a constant ratio to that across the photosphere.

These observations have an important bearing on the physical conditions obtaining inside sunspots. For instance it is often assumed † that it is the rapid upward motion of a gas, accompanied by adiabatic cooling, which gives rise to spot darkening. However, it appears to be impossible to explain the constant intensity ratio if the visible region is in adiabatic equilibrium.‡

Before considering various forms of motion which might produce the observed effects, it appears desirable to examine the effect of a mere difference of absorption coefficient between spot and disk. We proceed to do this by setting up the equations governing radiative equilibrium in an appropriate form.

2. Regarding a sunspot as a region of different absorption coefficient, we have to examine the equations governing radiative equilibrium in a spot.

Let the radiant energy crossing $d\sigma$ in time $dt$ lying inside $d\omega$ making an angle $\theta$ with the normal to $d\sigma$ be

$$I(\theta) \cos \theta d\sigma d\omega dt$$

so that $I(\theta)$ is the specific intensity.

The net flux across $d\sigma$ is then

$$\int_0^{2\pi} \int_0^{\pi} I(\theta) \sin \theta \cos \theta d\theta d\phi = F \text{ say,}$$

$$= \int I(\theta) \cos \theta d\omega \quad \text{since} \quad d\omega = \sin \theta d\theta d\phi.$$

---

* Wormell, *M.N.*, 96, 736, 1936; Moore, *Ap. J.*, 75, 222, 298, 1932.

† Russell, *Ap. J.*, 54, 293, 1921; Milne, *M.N.*, 90, 487, 1930.

‡ Minnaert and Wanders, *Z. Astrophys.*, 5, 297, 1932.

The energy crossing $d\sigma$ in time $dt$ lying inside $d\omega$ and making an angle $\theta$ with the normal to $d\sigma$ has momentum

$$(1/c)I(\theta)\cos\theta d\sigma d\omega dt,$$

so that the normal component of momentum across $d\sigma$ is

$$(1/c)d\sigma dt I(\theta)\cos^2\theta d\omega,$$

and thus the net transfer is

$$(1/c)d\sigma dt\int I(\theta)\cos^2\theta d\omega.$$

The radiation pressure $p_r$ is then given by

$$p_r=(1/c)\int I(\theta)\cos^2\theta d\omega.$$

To find the equation of radiant energy transfer consider an elementary cylinder of length $ds$, section $d\sigma$, and let $I(\theta)$ be the specific intensity of the radiation incident on one face, $I(\theta)+dI(\theta)$ the emergent intensity, both these latter being in the direction of $s$.

The energy lost inside the cylinder is

$$\kappa\rho I(\theta)d\omega d\sigma ds dt,$$

and the energy gained is

$$j\rho d\omega d\sigma dt ds,$$

where $\kappa, j$ denote the mass-absorption coefficient and emission coefficient respectively.

In the steady state then,

$$\frac{dI(\theta)}{ds}=\rho(j-\kappa I(\theta)).$$

It can be shown that for material in local thermodynamic equilibrium we should have

$$\frac{dI(\theta)}{ds}=\rho\kappa'(B-I(\theta)),$$

where $\kappa'$ is the Rosseland mean, and $B$ the (integrated) black-body intensity.

Multiply this equation by $d\omega$ and integrate over the complete sphere. We get div $\mathbf{F}=0$, where $\mathbf{F}$ is a vector whose components are $\int I(\theta)l d\omega$, etc., *i.e.* the flux, and it is assumed that there are no energy sources present. If, however, there are sources present then

$$\text{div } \mathbf{F}=\rho\epsilon,$$

where $\epsilon$ is the energy liberated per gm.

It can be shown, moreover, that

$$\mathbf{F}=-\frac{c}{\rho\kappa'}\text{grad } p_r. \tag{1}$$

Hence we see that in the outer layers, with $\kappa'$ constant, and assuming also that the density $\rho$ is constant throughout the region considered,

$$\text{div grad } p_r=0, \quad i.e. \quad \nabla^2T^4=0 \tag{2}$$

To determine the temperature distribution in a region containing a spot we have to solve this equation together with its boundary conditions. These are (i) that the temperature is continuous across the spot boundary; (ii) that the net flux is the same reckoned from both sides of this boundary; (iii) that the spot does not disturb conditions at a great distance; and finally that the net flux is unchanged (iv). If (iii) is satisfied so is (iv), since div $\mathbf{F}=0$ as shown above. We proceed to solve this problem, first for a hemispherical spot, then for spots in the shape of ellipsoids of revolution.

3. Consider a sphere in which the absorption coefficient is $k'/\rho'$ placed in an otherwise uniform radiation field, the material of which has absorption coefficient $k/\rho$.

Take the $x$-axis in the direction of the original field, and the origin of co-ordinates at the centre of the sphere. We seek solutions of Laplace's equation of the form

$$T^4 = RS \text{ say,}$$

where $R$ is a function of $r$ only, $S$ a function of $\theta$, $\phi$ only; $r$, $\theta$, $\phi$ being the usual spherical polar co-ordinates. In these co-ordinates $\nabla^2 V = 0$ becomes

$$\frac{\partial}{\partial r}\left(r^2\frac{\partial V}{\partial r}\right)+\frac{1}{\sin\theta}\frac{\partial}{\partial\theta}\left(\sin\theta\frac{\partial V}{\partial\theta}\right)+\frac{1}{\sin^2\theta}\frac{\partial^2 V}{\partial\phi^2}=0.$$

Put $V=RS$; then since we have circular symmetry about the axis of $x$, $\partial V/\partial\phi = 0$ and we get

$$0=\frac{1}{R}\frac{d}{dr}\left(r^2\frac{dR}{dr}\right)+\frac{1}{S\sin\theta}\frac{\partial}{\partial\theta}\left(\sin\theta\frac{\partial S}{\partial\theta}\right).$$

The first member is a function of $r$ only, the second a function of $\theta$ only, hence both must be constant. Thus we get

$$\frac{1}{R}\frac{d}{dr}\left(r^2\frac{dR}{dr}\right)=K \tag{3}$$

and

$$\frac{1}{S\sin\theta}\frac{\partial}{\partial\theta}\left(\sin\theta\frac{\partial S}{\partial\theta}\right)+K=0. \tag{4}$$

The most general solution of (3) is

$$R=Ar^n+Br^{-n-1} \quad \text{with} \quad K=n(n+1),$$

while (4) becomes

$$\frac{1}{S\sin\theta}\frac{d}{d\theta}\left(\sin\theta\frac{dS}{d\theta}\right)+n(n+1)=0$$

which is Legendre's equation of order $n$ in the variable $x'=\cos\theta$. Our general solution is accordingly

$$V=(Ar^n+Br^{-n-1})S_n,$$

where $A$, $B$ are arbitrary constants.

Originally the field is given by

$$T^4=T_0^4+Fx\ ;$$

suppose that inside the sphere

$$T_i^4=V_i=\alpha rS_1+T_0^4$$

while outside

$$V_0=rS_1+\frac{\beta S_1}{r^2}+T_0^4.$$

We have put $n=1$ in the general solution so as to satisfy boundary conditions (iii) and (iv).

Condition (ii) gives that

$$\frac{1}{k'}\frac{\partial V_i}{\partial r}=\frac{1}{k}\frac{\partial V_0}{\partial r} \quad \text{at} \quad r=a, \text{ the spot boundary.}$$

Thus we have, from (1), (ii)

$$\alpha a=a+\beta a^{-2}$$

$$\alpha k/k'=1-2\beta a^{-3},$$

so that

$$\alpha=\frac{3k'}{k+2k'},\qquad \beta=\frac{(k'-k)a^3}{(k+2k')}.$$

Furthermore $S_1$ satisfies

$$\frac{1}{\sin\theta}\frac{d}{d\theta}\left(\sin\theta\frac{dS_1}{d\theta}\right)+2S_1=0.$$

so that

$$S_1=F\cos\theta.$$

The solution is then

$$T^4=T_0^4+Fx\left(1-\frac{k-k'}{k+2k'}\frac{a^3}{r^3}\right)$$

outside the sphere and

$$T^4=T_0^4+\frac{3Fk'x}{k+2k'}$$

inside the sphere. (Note that if $k=k'$ we have $T^4=T_0^4+Fx$ as required.)

The most striking feature of the solution is that the radiation field inside the spot has the same direction as the undisturbed field. As a matter of observation it is a feature of sunspots that the energy flux is constant across the umbra. The model considered exhibits this property. Furthermore the flux just outside the spot is appreciably greater than that across the disk; this is the bright ring phenomenon. Surrounding the umbra in a typical spot is a lighter region, the penumbra. Our model can be made to incorporate this feature in the following way.

Suppose that the spot has an outer shell of absorption coefficient $k_1/\rho_1$, while the central region has absorption coefficient $k_2/\rho_2$.

Suppose that in the exterior region (of absorption coefficient $k/\rho$)

$$T^4=T_0^4+rS_1+\frac{\alpha S_1}{r^2},$$

and in the outer shell

$$T^4=\beta rS_1+\frac{\gamma S_1}{r^2},$$

and in the central region

$$T^4=\delta rS_1.$$

The two boundary conditions at the two interfaces give us four equations, and the final solution is

$$\frac{\gamma}{\beta}=\frac{k_2-k_1}{k_1+2k_2}b^3,\qquad \frac{\delta}{\beta}=\frac{3k_2}{2k_2+k_1}$$

with

$$\beta=\frac{3a^3k_1(k_1+2k_2)}{(k+2k_1)(2k_2+k_1)a^3+2(k_2-k_1)(k_1-k)b^3}$$

and $\alpha=a^3(\beta-1)+\gamma$ ($b$ the inner radius, $a$ the outer). We shall have constant flux in the umbra, and in addition there is a penumbra of different brightness.

From equation (1) we see that the flux across a region whose absorption coefficient is $k/\rho$ is proportional to

$$\frac{1}{k}\frac{\partial T^4}{\partial x}.$$

The variation of flux across the spot and the disk in the two cases discussed above is shown in Figs. 1 and 2.

For a hemispherical spot the ratio of the flux across the disk to the flux across the umbra is

$$\frac{k+2k'}{3k}.$$

According to actual measurement this ratio has the value 2 approximately so that $k'/k = 2{\cdot}5$.

The above treatment can be extended to the case where $k$ is a function of $r$, continuous or otherwise.

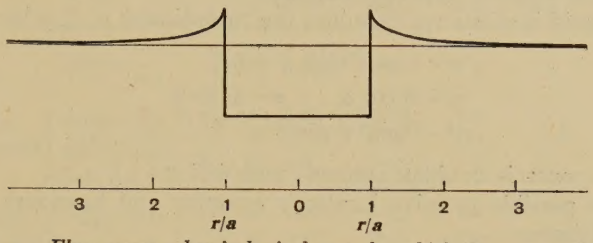


FIG. 1.—*Flux across a hemispherical spot, for which* $(k)_{\text{spot}} = 2{\cdot}5(k)_{\text{disk}}$.

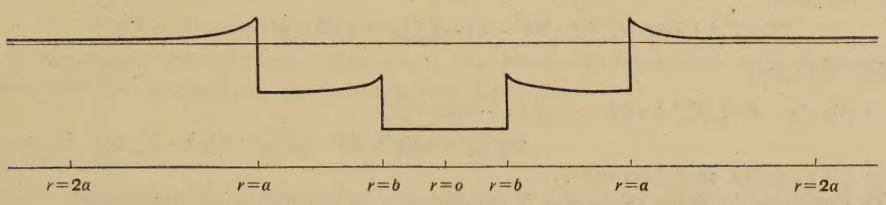


FIG. 2.—*Flux across a composite spot for which the radius of the penumbra is a, the radius of the umbra b, where* $a = 3b$, *and* $(k)_{\text{disk}}/(k)_{\text{penumbra}}/(k)_{\text{umbra}} = 1/2/5$. *The results correspond closely to those obtained from observation by Wormell,* loc. cit., *p.* 743.

4. In order to examine the effect of a variable depth-aperture ratio we consider the case of a spot whose shape is that of an ellipsoid of revolution, either prolate or oblate. Supposing the ellipsoid prolate, with the $x$-axis the major axis, and introducing the co-ordinates $\mu$, $\zeta$, $\rho$ by means of the equations:

$$x = l\cos\theta\cosh\eta \equiv l\mu\zeta,$$

$$y = \varpi\cos\rho, \qquad z = \varpi\sin\rho,$$

$$\varpi^2 = l^2\sin^2\theta\sinh^2\eta = l^2(1-\mu^2)(\zeta^2-1),$$

we have the surface $\zeta = \text{const.}$ is a prolate ellipsoid with foci at $(\pm l, 0, 0)$.

It is then possible to solve Laplace's equation, together with the appropriate boundary conditions by the method of separation of variables, the solution being

$$\{AQ_1(\zeta) + BP_1(\zeta)\}P_1(\mu)$$

outside the spot, and

$$aP_1(\zeta)P_1(\mu)$$

inside; the first order Legendre equations are chosen to satisfy the conditions at infinity, and thus the equation of continuity, as before. The remaining boundary conditions serve to determine the constants in the above expressions and we obtain finally that—inside the spot,

$$T^4 = T_0{}^4 + Fxk'[(\zeta_0{}^2-1)(k'-k) - \tfrac{1}{2}\zeta_0(\zeta_0{}^2-1)(k'-k)\log\{(\zeta_0+1)/(\zeta_0-1)\} + k']^{-1}$$

outside the spot,

$$T^4 = T_0{}^4 + Fx + Fx\zeta_0(\zeta_0{}^2-1)(k'-k)[\tfrac{1}{2}\log\{(\zeta+1)/(\zeta-1)\} - 1/\zeta]$$
$$\times[(\zeta_0{}^2-1)(k'-k) - \tfrac{1}{2}\zeta_0(\zeta_0{}^2-1)(k'-k)\log\{(\zeta_0+1)/(\zeta_0-1)\} + k')]^-$$

where $\zeta$ is given by

$$\frac{x^2}{l^2\zeta^2}+\frac{y^2+z^2}{l^2(\zeta^2-1)}=1,$$

and $\zeta=\zeta_0$ is the boundary of the spot. We again have the feature that the flux is constant across the surface of the spot.

It can be shown that the solution above approaches that given for the spherical spot when the axes of the ellipsoid approach equality.

When the ellipsoid is oblate we introduce the co-ordinates $\mu$, $\zeta$, $\rho$ by the relations:

$$x=l\cos\theta\sinh\eta\equiv l\mu\zeta$$
$$y=\varpi\cos\rho,\qquad z=\varpi\sin\rho$$
$$\varpi^2=l^2\sin^2\theta\cosh^2\eta$$

and the surface $\zeta=$ const. is an oblate spheroid with foci at $(\pm l, 0, 0)$.

As before it is possible to solve Laplace's equation and boundary conditions, the solution being as follows:—

inside the spot,

$$T^4=T_0^4+Fxk'[(\zeta_0^2+1)(k'-k)-\zeta_0(\zeta_0^2+1)(h-h')\cot^{-1}\zeta_0+k']^{-1}$$

outside the spot,

$$T^4=T_0^4+Fx-Fx\zeta_0(\zeta_0^2+1)(k'-k)\{(1/\zeta)-\cot^{-1}\zeta\}$$
$$\times[(\zeta_0^2+1)(k'-k)-\zeta_0(\zeta_0^2+1)(h-h')\cot^{-1}\zeta_0+k']^{-1},$$

where $\zeta=\zeta_0$ is the spot boundary.

The solution in these two cases is represented in the following diagrams.

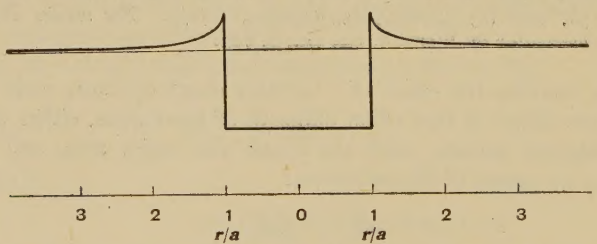


FIG. 3.—*Flux across a prolate spot, the major axis being double the minor, for which* $(k)_{\text{spot}}=2{\cdot}5(k)_{\text{disk}}$.

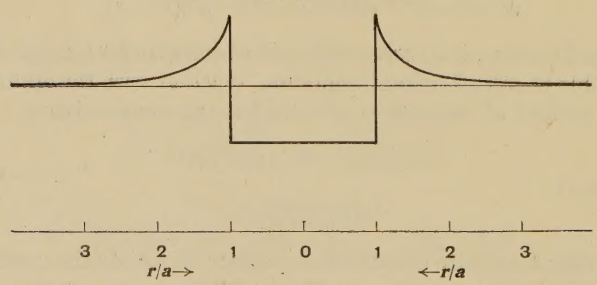


FIG. 4.—*Flux across a spot in the form of an oblate spheroid, with major axis twice the minor, and with* $(k)_{\text{spot}}=2{\cdot}5(k)_{\text{disk}}$.

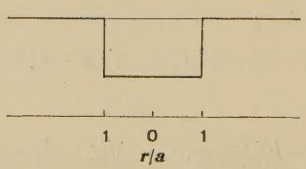


FIG. 5.—*Flux across a prolate spot of great depth, for which* $(k)_{\text{spot}}=2{\cdot}5(k)_{\text{disk}}$.

The ratio of the flux across the spot surface to the flux across the disk, for various values of $k_{\text{disk}}/k_{\text{spot}}$ is given in the following table.

TABLE I

*Ratio of flux across the spot surface to flux across the disk*

| Model | | $k_{\text{disk}}/k_{\text{spot}}$ 0 | 0·25 | 0·50 | 1·0 | 2·0 | 10·0 |
|---|---|---|---|---|---|---|---|
| sphere | | 0 | 0·33 | 0·6 | 1·0 | 1·5 | 2·5 |
| oblate spheroid | major axis = 2 | 0 | 0·63 | 0·83 | 1·0 | 1·11 | 1·22 |
| | major axis = 10 / minor axis | 0 | 0·71 | 0·88 | 1·0 | 1·08 | 1·14 |
| | minor axis = ∞ | 1 | 1·0 | 1·0 | 1·0 | 1·0 | 1·0 |
| prolate spheroid | major axis = 2 | 0 | 0·28 | 0·55 | 1·0 | 1·72 | 3·98 |
| | major axis = 10 / minor axis | 0 | 0·26 | 0·51 | 1·0 | 1·99 | 9·91 |
| | minor axis = ∞ | 0 | 0·25 | 0·50 | 1·0 | 2·0 | 10·0 |

5. According to the above discussion, the observed brightness ratio between the umbra and the photosphere can be explained if we have

$$k_{\text{spot}} = 2{\cdot}5 k_{\text{disk}}$$

approximately.

It it now generally accepted that the opacity of the outer layers of a star is due to absorption by negative hydrogen ions.* Hence the absorption coefficient is proportional to $n^-$, the number of negative hydrogen ions per c.c.

Since the detachment potential is small in comparison with $RT$, Saha's relation becomes

$$\frac{n_e n^+}{n^-} = \frac{2(2\pi m RT)^{3/2}}{h^3}\varpi$$

and we have, since

$$P_e = n_e RT,$$

that

$$n^- \propto \frac{P_e}{T^{5/2}}, \quad \text{so that} k \quad \propto \frac{P_e}{T^{5/2}}.$$

Miss Moore in her discussion of the observational data states values of $\rho$, $P_e$ for spot and disk.† From her work we have

$$\kappa_{\text{spot}} = 1{\cdot}25 \kappa_{\text{disk}} \text{ approximately and } \rho_{\text{spot}} = 1{\cdot}70 \rho_{\text{disk}} \text{ approximately,}$$

so that

$$k_{\text{spot}} = 2{\cdot}1 k_{\text{disk}}.$$

We conclude then that the observational results certainly do not exclude the possibility that the ratio $k_{\text{spot}}/k_{\text{disk}}$ is high enough to explain the observed contrast between the spot and the disk.

The writer is indebted to Dr. Woolley for suggesting this problem, and for discussions of the results.

*Commonwealth Observatory,*
*Mount Stromlo,*
*Canberra:*
1946 *January* 21.

* Wildt, *Ap. J.*, 90, 611, 1939.
† Moore, *loc. cit.*, pp. 321, 327.

# STELLAR OPACITY

*R. v. d. R. Woolley*

(Received 1945 November 2)

*Summary*

The stellar absorption coefficient is considered as arising from a number of classical oscillators. It is assumed that, leaving out consideration of possible ionization, there are $\phi(\nu)d\nu$ oscillators with critical frequencies between $\nu$ and $\nu+d\nu$. The Rosseland mean opacity is then calculated allowing for ionization of the oscillators and it is shown that if $\phi(\nu) \propto \nu^{-n}$, $k_2 \propto \rho T^{-(\frac{7}{2}+n)}$ for giant stars and $k_2 \propto T^{-n}$ for dwarf stars. It is suggested that $n=0$ may be a good approximation to the actual distribution of oscillators.

---

1. The great advances which have been made in nuclear physical theory in the last decade hold out considerable promise of a corresponding advance in the theory of the internal constitution of the stars. It has been necessary up to the present to assume various laws for the distribution of energy generation within a star, and these assumptions may soon be replaced by well-founded physical laws. It is therefore appropriate to examine the theory of stellar opacity at the present moment, more especially as it is known that in at least one case of energy distribution, the point source model, heavy numerical calculations are required, in which it is necessary to assume a formula for the behaviour of the stellar opacity as a function of temperature and pressure.

Eddington's classical papers on stellar opacity are summarized in *The Internal Constitution of the Stars*, where the important "Rosseland mean" * is adopted. A different derivation of the opacity from Kramers' law has been given by Milne † and an important paper by Chandrasekhar ‡ arrives at the conclusion, among others, that "A study of the absorption coefficient shows that a law of the type $k \propto \rho T^{-7/2}$ is not very reliable, and this fact has to be specially emphasized since very many numerical integrations such as have been carried out by Strömgren, Biermann and others lose much of their quantitative interest in view of the lack of any really reliable evaluation of the coefficient of opacity."

While Eddington in *The Internal Constitution of the Stars* saw no reason to suspect his result, $k \propto \rho/\mu T^{7/2}$, he was at the time concerned over the fact that the value of the constant of proportionality in this relation deduced from astronomical evidence was about ten times the theoretical value. He remarked: "If Kramers' theory were merely a speculation as to the manner in which classical laws pass over into quantum laws, it would not greatly disturb us to find astronomical results partly discordant with it. But the theory has been compared with laboratory experiments and found satisfactory, so that astronomical conflict with Kramers' theory is virtually a conflict with laboratory experiment". The particular conflict was shown by Strömgren § and Eddington || to be resolved when the hydrogen abundance in the stellar interior is adjusted from the value originally adopted by Eddington to the value estimated by Russell from stellar spectra. Eddington's remark, however, suggests that a well-founded theory of stellar opacity

* Rosseland, *M.N.*, 84, 525, 1925.
† *M.N.*, 85, 750, 1925.
‡ *Proc. Roy. Soc.*, A, 135, 472, 1932.
§ *Z. Astrophys.*, 4, 118, 1932.
|| *M.N.*, 92, 47, 1932.

might be derived from the empirical facts of X-ray spectra. These are very simple. For an element of atomic number $Z$ the absorption coefficient for the $K$ electrons is $a_K = 0{\cdot}020 Z^4\lambda^3$, and for the $L$ electrons $a_L = 0{\cdot}003 Z^4\lambda^3$. In both cases the coefficient is zero if $\lambda$ is greater than the wave-length of the absorption edge of the spectrum in question.

2. We can express these empirical laws in terms of oscillator strengths. The continuous spectrum at the head of a series whose limiting frequency is $\nu_0$ and whose absorption coefficient follows a $\lambda^3$ law has an absorption coefficient $a(\nu)$ where

$$a(\nu) = \lambda^3 \times \frac{2\pi e^2 \nu_0^2}{mc^4} \times f_c$$

and $f_c$ is the oscillator strength of the continuous spectrum.* Now for a hydrogen-like spectrum of principal quantum number $n$

$$\nu_0^2 = 4\pi^4 m^2 e^8 Z^4/(h^6 n^4),$$

so that the proportionality of $a_K$ and $a_L$ to $Z^4\lambda^3$ simply means that the oscillator strengths of the $K$ spectra are all equal, from atom to atom. Similarly the oscillator strengths of the continuous spectra are all equal. Since for heavy atoms there are two $K$ levels for which $n = 1$ and eight $L$ levels for which $n = 2$, the empirical results show that the oscillator strengths of the individual $L$ levels are about half those of the individual $K$ levels. The two $K$ levels taken together have an oscillator strength equal to unity. Now we may regard the stellar atmosphere as an assembly of oscillators. Disregarding the distinction between $K$ and $L$ oscillators, the absorption coefficient of the atmosphere as a whole for any wave-length $\lambda$ is obtained by summing all the contributions made by all the oscillators which are capable of absorbing $\lambda$, namely those for which $\nu_0 < c/\lambda$. Now let us suppose that under given conditions there are $f(\nu)d\nu$ oscillators per gm. of the atmosphere having their limiting frequencies $\nu_0$ between $\nu$ and $\nu + d\nu$. Then the absorption coefficient per gm. of the atmosphere is

$$\lambda^3 . \frac{2\pi e^2}{mc^4} \int_0^{c/\lambda} \nu^2 f(\nu) d\nu.$$

If we knew the constitution of the atmosphere, and if we knew from X-ray spectroscopy all the absorption edges and the oscillator strengths attached to each, we could construct the function $f(\nu)$ from purely empirical data. Allowance must of course be made for the state of ionization of the various atoms in the atmosphere. Failing an empirical construction of $f(\nu)$ we may explore the position by separating $f(\nu)$ into two factors, one depending on the occurrence of oscillators of frequency $\nu$ to $\nu + d\nu$ regardless of ionization and the other representing the state of ionization of the typical ion with ionization potential $\chi = h\nu$. To simplify the analysis we shall suppose that in each case only two states of ionization are present in the atmosphere, the oscillator arising from a transition between these states.

If there are $n(1 - x)$ ions of a particular kind and $nx$ ions of the same atom with one less electron, both per c.c., and if there are $n_e$ electrons per c.c. then

$$n_e x/(1 - x) = \varpi . 2(2\pi mRT)^{3/2} h^{-3} e^{-\chi/kT} = K(\chi, T), \qquad (2.1)$$

where $\varpi$ is a weight factor of order unity. Then

$$1 - x = \frac{n_e}{n_e + K(\chi, T)}.$$

Of the $n$ atoms the fraction $(1 - x)$ has its limiting frequency $\nu_0$ at $\nu = \chi/h$.

* Cf. *M.N.*, 95, 101, 1934.

Under these circumstances

$$f(\nu)=\phi(\nu)\times\frac{n_e}{n_e+K(\chi,\ T)},$$

where $\phi(\nu)$ represents the distribution of oscillators regardless of ionization.

Then if $k(\nu)$ is the absorption coefficient per gm. of the atmosphere

$$\nu^3k(\nu)=\frac{2\pi e^2}{mc}\int_0^\nu\frac{n_e\nu^2\phi(\nu)d\nu}{n_e+K(h\nu,\ T)}. \tag{2.2}$$

The stellar opacity $k_2$ is given by the "Rosseland mean" or

$$\frac{1}{k_2}=\int\frac{1}{k(\nu)}\frac{\partial B(\nu,\ T)}{\partial T}d\nu\Big/\int\frac{\partial B(\nu,\ T)}{\partial T}d\nu,$$

where $B(\nu,\ T)=C\nu^3(e^{h\nu/RT}-1)^{-1}$. Since 70 per cent. of the weight of the Rosseland mean lies between $h\nu/RT=2{\cdot}5$ and $h\nu/RT=7$, we may with sufficient accuracy take $B(\nu,\ T)=C\nu^3e^{-h\nu/RT}$, giving

$$\frac{1}{k_2}=\int\frac{1}{k(\nu)}\nu^4e^{-h\nu/RT}d\nu\Big/\int\nu^4e^{-h\nu/RT}d\nu. \tag{2.3}$$

We can calculate the opacity $k_2$ from (2.2) and (2.3) if we assume that $\phi(\nu)=b\nu^{-n}$. In the next section we examine cases of special interest.

3. (A) If $n=0$ and $\phi(\nu)=b$, we have

$$\nu^3k(\nu)=\frac{2\pi e^2b}{mc}\int_0^{h\nu/RT}\left(\frac{RT}{h}\right)^3\frac{x^2dx}{1+ae^{-n}},$$

where $a=\varpi.2(2\pi mRT)^{3/2}/(h^3n_e)$.

If now $a$ is so small that $ae^{-x}$ may be neglected in the integral for the most important values of $h\nu/RT$, namely from $h\nu/RT=2{\cdot}5$ onwards,

$$\int_0^{h\nu/RT}\frac{x^2dx}{1+ae^{-x}}=\tfrac{1}{3}\left(\frac{h\nu}{RT}\right)^3,$$

so that $k(\nu)=\frac{2}{3}\dfrac{\pi e^2b}{mc}$, and is independent of $\nu$ and $T$. Again if $a$ is so large that $ae^{-x}>>1$ in the important range of the integral,

$$\int_0^a\frac{x^2dx}{1+ae^{-x}}=\frac{1}{a}\int_0^a x^2e^xdx\approx\frac{1}{a}a^2e^a.$$

In this case, from (2.3)

$$k_2=\frac{2^6}{5}\cdot\frac{\pi e^2b}{mc}\cdot\frac{h^3n_e}{(2\pi mRT)^{3/2}}$$

or if $n_e\propto\rho$, which would be the case with hydrogen preponderating, $k_2\propto\rho T^{-3/2}$. An important consequence of this is that in Eddington's standard model $\rho T^{-3/2}$ decreases strongly going outwards, so that "$k\eta=$constant" becomes absurd.

(B) The case $n=2$ is of interest because from it we can recover Eddington's form $k_2 \propto \rho T^{-7/2}$. Let $\phi(\nu)=\psi\nu^{-2}$. Then $\nu^2\phi(\nu)d\nu=\psi d\nu$ and

$$\int_0^{\nu} \frac{\nu^2\phi(\nu)d\nu}{1+K/n_e}=\frac{RT}{h}\int_0^{h\nu/RT}\frac{\psi dx}{1+ae^{-x}}=\frac{RT\psi}{h}\ln\left(\frac{e^{h\nu/RT}+a}{1+a}\right).$$

With $a$ small we have $\ln\left(\frac{e^{h\nu/RT}+a}{1+a}\right)=\frac{h\nu}{RT}$ and $\nu^3k(\nu)=\frac{2\pi c^2}{mc}.\psi\nu$. Then from (2.3)

$$k_2=\frac{2\pi e^2}{mc}\frac{1}{7.6}\psi\left(\frac{h}{RT}\right)^2,$$

so that $k_2 \propto T^{-2}$, independent of $\rho$.

On the other hand if $a$ is large we have

$$\ln\left(\frac{e^{h\nu/RT}+a}{1+a}\right)\longrightarrow\frac{1}{a}e^{h\nu/RT},$$

$$\nu^3k(\nu)=\frac{2\pi e^2}{mc}\frac{RT\psi}{ha}e^{h\nu/RT},$$

$$k_2=\frac{2\pi e^2\psi}{mc}\frac{2^8}{7.6.5}\frac{h^5n_e}{2(2\pi m)^{3/2}(RT)^{7/2}},$$

so that in this case $k_2 \propto n_eT^{-7/2}$.

(C) Chandrasekhar finds $k \propto \rho T^{-9/2}$ (or $\rho_eT^{-11/2}$) as a straight mean (not a Rosseland mean) of the absorption due to a single oscillator by "neglecting small variations in ionisation". This step is legitimate if the element is mainly "ionized" or $x \approx 1$. In this case $1-x=h^3n_ee^{\chi/RT}/2(2\pi mRT)^{3/2}$. The straight mean gives

$$k_1=\int_{\nu_0}^{\infty}k(\nu)B(v,\,T)d\nu\Big/\int_{\nu_0}^{\infty}B(\nu,\,T)d\nu.$$

For a single oscillator $k(\nu)=\frac{2\pi e^2{\nu_0}^2}{3mc}\cdot\frac{f}{\nu^3}\cdot(1-x)$, leading to

$$k_1=n_eT^{-9/2}\times\frac{10e^2{\nu_0}^2f}{\pi^3mc}\cdot\frac{h^6}{2(2\pi m)^{3/2}R^{9/2}}$$

or $k_1 \propto n_eT^{-9/2}$. The single oscillator gives a zero Rosseland mean since $k(\nu)$ is zero for certain values. The law $k_2 \propto n_eT^{-9/2}$ corresponds to $\phi(\nu) \propto \nu^{-3}$, and of course $x \approx 1$ corresponds to $a$ large.

4. Using Eddington's data as shown in *The Internal Constitution of the Stars*, but choosing $\mu=1$ to fit later estimates of hydrogen abundance and taking $n_e=\frac{2}{3}\frac{\rho}{H}$ to suit $\mu=1$, we find for the central conditions in various stars the following values:—

| | $M$ | $1-\beta$ | $\rho_c$ | $T_c$ | $n_e$ | $a$ |
|---|---|---|---|---|---|---|
| *Capella* | 4·18 | 0·045 | 0·123 | $5{\cdot}7.10^6$ | $4{\cdot}95.10^{22}$ | 1347 |
| Sun | 1 | 0·00305 | 76·5 | $19{\cdot}6.10^6$ | $3{\cdot}06.10^{25}$ | 13·8 |
| Kr 60 | 0·27 | 0·00023 | 493 | $15{\cdot}5.10^6$ | $1{\cdot}98.10^{26}$ | 1·50 |

For a polytrope of index 3 we have $a \propto T^{3/2}\rho^{-1} \propto \mu^{-3/2}$. Since $h\nu/RT=4{\cdot}5$ is the centre of gravity of the Rosseland mean, the quantity $ae^{-4\cdot5}$ shows whether $a$ is to be regarded as large or small. The values of $ae^{-4\cdot5}$ for different values of the reduced radius $z$ are as follows:—

| $z$ | 0 | 1 | 2 | 3 | 4 | 5 |
|---|---|---|---|---|---|---|
| *Capella* | 15·0 | 18·9 | 33·7 | 69·5 | 157 | 404 |
| Sun | 0·154 | 0·194 | 0·346 | 0·714 | 1·61 | 4·2 |
| Kr 60 | 0·017 | 0·021 | 0·048 | 0·078 | 0·175 | 0·452 |

Accordingly $a$ may be considered large in *Capella* and small in Kr 60, and small in the centre of the Sun. The distinction is between stars in which levels with ionization potential $\chi = 4{\cdot}5RT$ are mainly unoccupied (*Capella*) or mainly occupied (Kr 60). We may summarize our results by saying that in giant stars the (Rosseland mean) opacity $k_2$ is proportional to $\rho T^{-(\frac{9}{2}+n)}$ and in dwarf stars it is proportional to $T^{-n}$, where $n$ is the index in the distribution law for oscillators, $\phi(\nu) = b\nu^{-n}$.

Inspection of the Table of Energy Levels shown in *The Internal Constitution of the Stars*, p. 252, suggests that $n = 0$, or $\phi(\nu)$ constant, may be a fair approximation to the actual distribution of energy levels of the oscillators. (For the lower $K$ levels (or lowes $L$ levels) alone, $n = -\frac{1}{2}$ if the elements are equally represented.)

*Commonwealth Observatory,*
*Mount Stromlo,*
*Canberra :*
1945 *October* 25.

# ON THE EXCITATION OF THE CORONAL SPECTRUM

*R. v. d. R. Woolley and S. C. B. Gascoigne*

(Received 1945 December 12)

*Summary*

The number of *Fe*XIV particles in the corona is counted and the number of recombinations $FeXIV + e \rightarrow FeXIII$ computed to be of order $10^{34}$ per second in the entire corona. It is calculated that if the *Fe*XIV ions are fission products arising from captures of neutrons by uranium atoms, at least $10^{40}$ neutrons must be captured by protons per second. This process would release about ten times the observed solar output of energy. It is concluded that Saha's theory that the *Fe*XIV lines observed in the corona are by-products of *U* fission cannot be sustained. Evidence for a coronal temperature of order $10^6$ degrees as suggested by Lyot is reviewed. No thermodynamical objection to the high temperature exists provided that a suitable source of energy can be found, and it is suggested that radio-active elements produced in the deep interior of the Sun and transported to the surface in disturbed solar areas provide a possible source.

---

1. Edlén's remarkable identifications of the coronal lines * have naturally led investigators to inquire how it is that ions having an ionization potential of more than 200 volts can exist in large numbers in the solar corona. The electron population in the inner corona is of order $4.10^8$ electrons per c.c., and if the corona were in thermodynamical equilibrium at 6000°, ions with a potential of about 15 volts would be half-ionized to the next stage of ionization, while ions with a potential of 200 volts would be present in negligibly small numbers.

To account for the presence of these highly ionized atoms, Lyot and others have suggested that the temperature of the corona is of order $10^6$ degrees. There are obvious difficulties connected with the maintenance of such temperatures at the surface of the Sun, and to avoid these Saha supposed † that the highly ionized atoms which Edlén's identifications demand, notably *Fe*XIV, are derived from products of nuclear fissions occurring in the Sun, induced by the bombardment of heavy atoms by neutrons. The present paper subjects Saha's theory to a numerical test and shows that it cannot be maintained as it stands. A modification of Saha's theory is suggested, in which the high state of ionization is attributed to collisions between *Fe* atoms and high energy fission products. This modification is similarly untenable. A further suggestion is made, that the corona is, as suggested by Lyot, actually at a much higher temperature than 6000°, and that this temperature is maintained by energy resulting from the disintegration of radio-active atoms produced in the Sun's interior and carried to the surface. This second modification seems at least tenable.

2. According to Lyot ‡, the intensity of the coronal line at 5303 A. at a distance of 35″ from the limb of the Sun is equal to $1{\cdot}2 \times 10^{-4}$ of the energy contained in 1 A. of the solar spectrum at the same wave-length. This figure, obtained by observation of the corona without eclipse, agrees well with an estimate made from Grotrian's observations at the eclipse of 1929.§

* Swings, *Ap. J.*, **98**, 116, 1943.

‡ *M.N.*, **99**, 580, 1939.

† *Proc. phys. Soc.*, **57**, 271, 1945.

§ *Z. Astrophys.*, **7**, 26, 1933.

According to Grotrian's observations all coronal emission lines, including the line at 5303 A. in particular, exhibit a maximum intensity at an angular distance of about 1′ from the limb. Most coronal line intensities fall off very sharply inside this maximum. Our object is to deduce the number of quanta emitted per second per c.c. of the corona from the observed intensity of the line. For this purpose let us suppose that the emission per c.c. per sec. with solid angle $d\omega$ is

$$Aa^n/r^n \cdot \frac{d\omega}{4\pi}$$

for $r > a$, and zero for $r < a$, where $r$ is the distance from the centre of the Sun. Then if we integrate along a column of unit cross-section in the line of sight tangential to the sphere of radius $r$ the amount emitted into solid angle $d\omega$ is

$$\frac{Aa^n}{r^{n-1}} \cdot \frac{\Gamma(\frac{1}{2})\Gamma\left(\frac{n-1}{2}\right)}{\Gamma\left(\frac{n}{2}\right)} \frac{d\omega}{4\pi}.$$

From Grotrian's diagram for 5303 A. we find that the emission drops off about one magnitude from 1′·1 outside the limb to 2′·6 outside the limb, giving $n = 11$. With this figure the emission into $d\omega$ at the maximum $r = a$ is

$$0{\cdot}813 \times Aad\omega/4\pi.$$

Now the Sun's total emission per sec. is $3{\cdot}780 \times 10^{33}$ ergs. If the solar energy curve is assumed to be a black-body curve with a colour temperature $T_c$ then the number of quanta emitted per square cm. of the Sun's surface per second into all outward directions in 1 A. of the spectrum at 5303 A. is

$$2{\cdot}592 \times 10^{35} \times T_c^{-4} \cdot \left(\exp \frac{h\nu}{RT_c} - 1\right)^{-1}.$$

Assuming a colour temperature $T_c = 6800°$ we get $2{\cdot}332 \times 10^{18}$ quanta per sq. cm. per sec. (The corresponding figure for $T_c = 6000°$ is $2{\cdot}183 \times 10^{18}$.) Of this the fraction $\frac{d\omega}{2\pi}$ is emitted within solid angle $d\omega$. We now have from Lyot's observation

$$0{\cdot}813 \times Aa(d\omega/4\pi) = 1{\cdot}2 \times 10^{-4} \times 2{\cdot}33 \times 10^{18} \times d\omega/2\pi,$$

and since $a = 6{\cdot}95 \times 10^{10}$ cm. we get

$$A = 10^4 \text{ quanta per c.c. per sec., very nearly.}$$

3. Edlén identifies the coronal line at 5303 A. with the " forbidden " transition

$$^2P^\circ_{\frac{3}{2}} \longrightarrow {}^2P^\circ_{\frac{1}{2}}$$

of *Fe*XIV. Quanta in this line might be emitted by one of two processes, (*a*) by capture and cascade

$$Fe\text{XV} + e \longrightarrow Fe\text{XIV}\ (^2P^\circ_{\frac{3}{2}}),$$
$$^2P^\circ_{\frac{3}{2}} \longrightarrow {}^2P^\circ_{\frac{1}{2}} + h\nu,$$

or (*b*) by scattering of sunlight by *Fe*XIV atoms in the $^2P^\circ_{\frac{1}{2}}$ state,

$$^2P^\circ_{\frac{1}{2}} + h\nu \rightleftharpoons {}^2P^\circ_{\frac{3}{2}}.$$

To examine the relative frequency with which these processes occur let us suppose that there are $n_1$ atoms of *Fe*XV at some point in the corona and the same number of *Fe*XIV atoms per c.c. (The relative populations of these ions will depend on their cross-

sections for electron capture, which will be roughly equal.) If $\alpha$ is the recombination coefficient and $n_e$ the number of electrons per c.c. there will be $\alpha n_e n_1$ recombinations per c.c. per second. Now $n_e$ is of order $4.10^{+8}$ in the inner corona, according to Baumbach *, and the value of $\alpha$, which will be discussed later, probably lies between $10^{-10}$ and $10^{-11}$. Hence there are not more than $4 \times 10^{-2} \times n_1$ recombinations per c.c. per second.

The Einstein transition coefficient $b_{21}$ for $^2P^\circ_{\frac{3}{2}} \rightarrow {}^2P^\circ_{\frac{1}{2}}$ in *Fe*XIV is 60 sec.$^{-1}$, according to Kun Huang.† The number of quanta scattered per sec. from a field of radiation density $\rho(\nu)d\nu$ is

$$n_1 . a_{12} . \rho(\nu),$$

where $a_{12} = b_{21} . \frac{q_2}{q_1} . \frac{c^3}{8\pi h\nu^3}$. Here $q_1$, $q_2$ are statistical weights and in this case $q_1 = 2$, $q_2 = 4$.

The radiation density in the inner corona may be taken from the number of quanta emitted per sq. cm. per sec. from the Sun, which we have taken to be $2{\cdot}33 \times 10^{18}$ in an interval of 1 A., giving $2{\cdot}2 \times 10^7$ in unit frequency interval. The radiation density is $\rho(\nu) = 5{\cdot}5 . 10^{-15}$, giving $n_1 a_{12} \rho(\nu) = 0{\cdot}58 n_1$, showing that process (*b*) is much more frequent than (*a*).

In the previous section we found that $10^4$ quanta were emitted per c.c. per sec.: since this number is equal to $0{\cdot}58 n_1$ we must have

$$n_1 = 1{\cdot}7 . 10^4.$$

This is the maximum concentration of *Fe*XIV ions per c.c. of the corona. It is worth noting that this figure agrees well with the abundance of *Fe* in the photosphere. According to Russell there is one *Fe* atom to about $2.10^4$ hydrogen atoms in the photosphere.‡ Now at that level in the corona with which we are concerned, there are $4.10^8$ electrons per c.c. according to Baumbach, and hence $4.10^8$ protons if the corona is electrically neutral. We should accordingly expect $2.10^4$ *Fe* atoms in all stages of ionization, which agrees well with our figure of $1{\cdot}7 . 10^4$ in the XIV stage, which is *observed* to give the strongest lines.

In calculating this figure for $n_1$ we have neglected the effect of electron collisions, which as shown by Hebb and Menzel § may become important in the excitation and de-excitation of forbidden lines. It should be emphasised here that we are concerned not so much with the excitation mechanism as with the population of *Fe*XIV $^2P^\circ_{\frac{1}{2}}$, that is, with $n_1$. Let $n_2$ be the density of *Fe*XIV $^2P^\circ_{\frac{3}{2}}$. Then if only radiative processes are effective,

$$n_1/n_2 = b_{21}/a_{12}\rho(\nu) = 103,$$

while if only collision processes are effective a Boltzmann distribution will result and at 6000° we shall have

$$n_1/n_2 = (q_1/q_2) . e^{h\nu/RT} = 47,$$

where $n_2$ is the observed density. Hence the deduced values of $n_1$ will not be very dependent on the particular mechanism.

Edlén pointed out that if collisional de-excitations were predominant, a Boltzmann distribution would result and the line intensities in a given ion would be proportional to $(2\mathcal{J}+1)Ave^{h\nu/RT}$. At 6000° the intensity ratio of the *Fe*XIII transitions $^1D_2 - {}^3P_2$, $^3P_2 - {}^3P_1$, $^3P_1 - {}^3P_0$ would then be 0·13 : 5·5 : 42. The observed ratios for the corresponding coronal lines $\lambda\lambda$ 3388, 10790 and 10747 are 16 : 35 : 55. We infer that *in a 6000° corona,* collisional de-excitation, and hence collisional excitation, are unimportant in comparison with the corresponding radiative processes.

* Quoted in Unsöld, *Physik der Sternatmosphären*, p. 440, Berlin, 1938.

† *Ap. J.*, **101**, 187, 1945. ‡ *Ap. J.*, **70**, 11, 1929. § *Ap. J.*, **92**, 408, 1940.

4. We now wish to count the number of recombinations

$$Fe\text{XIV} + e \rightarrow Fe\text{XIII}$$

which occur per second in the entire corona. The number which occur in each c.c. is $\alpha n_e n_1$ per second. Let us suppose that

$$n_e = B(a/r)^p,$$
$$n_1 = C(a/r)^q,$$

both expressions holding for $r > a$. Then the total number of recombinations which occur is

$$N = \frac{4\pi a^3}{p+q-3} \times \alpha BC.$$

It is clear that as far as the order of magnitude is concerned, the precise values of $p$ and $q$ are not very important. Since the inner corona emits most of the quanta, it is better to take $p = q = 10$ rather than use "Turner's law" $n \propto r^{-6}$ which applies to the *outer* corona. $B$ and $C$ are of course the values of $n_e$ and $n_1$ at the maximum (of $n_1$), $r = a$. We have seen that $C = 1{\cdot}7 \times 10^4$. From Baumbach's analysis, $B$ may be taken as $4 \times 10^8$ electrons per c.c.

The value of $\alpha$ requires discussion. According to wave mechanics, the cross-sections $\sigma$ for capture or excitation processes between atoms and free electrons vary, for hydrogen-like atoms and not too large electron velocities, as $Z^2v^{-2}$, where $Ze$ is the charge of the ion and $v$ the velocity of the electron. We may write generally $\sigma = AZ^2v^{-2}$, where $A$, roughly speaking, depends only on the electron configuration of the ion and the state into which the electron is captured. Assuming a Maxwellian distribution of electron velocities defined by a temperature $T$, the number of collisions between ions and electrons with velocities between $v$ and $v + dv$ is

$$\frac{4}{\sqrt{\pi}} AZ^2 n_e n_1 \left(\frac{m}{2RT}\right)^{\frac{3}{2}} \exp\left(-\frac{mv^2}{2RT}\right) v\, dv,$$

where $n_1$ is the density of the ions and $n_e$ of the electrons. Integrating over the velocities, we have for the total number of collisions per second

$$AZ^2 n_e n_1 (2m/\pi RT)^{\frac{1}{2}}.$$

The recombination coefficient $\alpha$ is therefore given in terms of the cross-section by

$$\alpha = AZ^2(2m/\pi RT)^{\frac{1}{2}}.$$

Huang gives $4{\cdot}1\ 10^{-4}$ for $AZ^2$ for the capture of electrons into the $^2P^\circ_{\frac{3}{2}}$ state of $Fe$XIV. At 6000° the corresponding $\alpha$ is $1{\cdot}1\ .\ 10^{-11}$. If we estimate $\alpha$ for $Fe$XIV from the value for $O$, calculated by Bates, Buckingham, Massey and Unwin *, which is $0{\cdot}4 \times 10^{-12}$ for 6000°, and multiply by the square of the charge, we get $8.10^{-11}$ for $Fe$XIV, nearly.

Adopting the lower figure for $\alpha$ (although the treatment by Bates *et al.* is probably to be preferred) we get

$$N = 2.10^{34}$$

recombinations per second, very nearly.

This is the number of $Fe$XIV particles which are removed from the corona per second by recombination. On Saha's theory they are replaced by $Fe$ atoms in a higher state of ionization ejected from the photosphere. Half the products of fission go inwards into the Sun: each fission cannot possibly produce more than *four Fe* nuclei, so that the minimum number of fissions which must occur per second to replace the $Fe$XIV ions in the corona is

$$\tfrac{1}{2}N \times 10^{34}.$$

* *Proc. Roy. Soc.*, A, 170, 322, 1939.

5. Although the cross-section for the capture of neutrons by $U$ is about 50 times the cross-section for capture of neutrons by protons under solar conditions, the probability of the capture of a neutron by a proton is much greater than the probability of capture by a nucleus of $U$ in the solar atmosphere, simply because hydrogen is much more abundant than uranium. In fact uranium has not been identified at all in the solar spectrum. Russell * gives the following estimates for the logarithms (to base 10) of the relative numbers of some of the elements:—

| | | | |
|---|---|---|---|
| *H* | 11·5 | *Fe* | 7·0 |
| *Na* | 7·2 | *Sr* | 3·3 |
| *Mg* | 7·4 | *Ba* | 3·3 |
| *Si* | 5·7 | *W* | 0·2 |
| *Ca* | 6·6 | *Pt* | 1·6 |
| *Ti* | 5·7 | *Pb* | 1·2 |

It seems safe to conclude that if the logarithm of the number of atoms has been as high as 3·5 on this scale the element would certainly have been identified. If this is so there are at least $10^8$ protons for each uranium atom in the solar atmosphere, and the probability that a neutron will be captured by a proton is at least $10^6$ times the probability that it will be captured by $U$. If, then, $10^{34}$ fissions take place per second, at least $10^{40}$ captures of neutrons by protons take place per second, according to the reaction

$$_1H^1 + {}_0n^1 = {}_1D^2 + 2{\cdot}15MV.$$

Since $1MV = 1{\cdot}59 \times 10^{-6}$ ergs, the total energy released per second by $10^{40}$ such reactions is $3{\cdot}5 \times 10^{34}$ ergs. This is ten times the total output of solar energy, and as it stands leads to the conclusion that nuclear fissions cannot take place in sufficient numbers to replace the *Fe*XIV particles lost by recombination in the corona.

The figure $3.10^{34}$ ergs may, moreover, be considered extremely low on several counts. It seems hardly likely that $U$, if present at all, can be more abundant than, say, *Pb*. Again, in assuming that each fission produces four *Fe* atoms, the maximum number permitted by the masses, we are making the most favourable possible assumption for Saha's theory. In fact *Fe* has not been observed at all as a product of $U$ fission, although by 1939 fifteen other elements had been so observed.† At a reasonable estimate either of these factors would increase one hundred-fold the figure we have deduced for the output of energy per *Fe* recombination in the corona. Other difficulties remain. The upper limit of the range of fission products is of order 30 cm. of hydrogen at N.T.P., so that if, as we have assumed, only those fissions occur which supply *Fe* atoms to the corona, these fissions and therefore the neutrons producing them must be confined to a *very thin sheet* of the photosphere. It seems unavoidable that this would require an extra-solar source of energy producing the neutrons, such as, for example, cosmic rays. The source would need to be of such a nature as to admit explanation of observed correlations between coronal and other solar phenomena. Moreover, extra-solar rays of sufficient quantity to produce the number of neutrons required could hardly fail to produce also very large effects in planetary atmospheres. Finally, any appreciable fraction of the solar energy released in a very thin sheet near the surface of the Sun would modify profoundly the radiative equilibrium of the photosphere. The theory which assumes no sources of energy in the photosphere agrees well with the observed darkening of the limb.

6. One may stave off some of the objections to the fission theory by supposing that the *Fe*XIV ions seen in the corona are not themselves the products of fission, but are *Fe* atoms normally present in the corona and raised from a low state of ionization by collision with fission products. A fission reaction which releases 40 *MV* has enough

* *Ap. J.*, **70**, 11, 1929. *Cf.* Unsöld, *loc. cit.*, p. 346.
† Walke, *Reports on Progress in Physics*, vi, 38, 1939.

energy to ionize $10^4$ *Fe* ions with a potential of 400 volts. Hence *if all the energy released in the fission process is devoted to ionizing Fe to FeXV*, the $2.10^{34}$ recombinations per second in the corona require $2.10^{30}$ fissions per second. If we now suppose that *U* is only as abundant as *Pb* we shall have $10^8$ proton-neutron reactions for every fission, or $2.10^{38}$ captures of neutrons by protons in each second. The energy released is $7 \times 10^{32}$ ergs per second, or about one-fifth of the total solar output. This energy must be released in a thin sheet near the surface, and it may safely be said that the hypothesis is untenable. If it be considered that the uranium concentration has possibly been taken unduly low, it must be remembered that only a small fraction of the fission energy could be devoted to ionizing *Fe*. Most of this energy would be dissipated by elastic collisions with other elements, particularly with hydrogen, so that the fission process would become a general source of heat rather than a specific source of *Fe*XIV. In this case, the concurrent capture of neutrons by protons is a far more prolific source of energy (actually of $2{\cdot}15MV\gamma$ radiation), so that from the point of view of the *Fe* ionization the presence or absence of *U* is of little consequence.

Can we then adopt Lyot's suggestion that the corona is at a very high temperature, and postulate neutron-proton reactions as the source of this temperature? The chief difficulties are associated with the neutrons, which would still have to be confined to a thin outer layer to ensure that only the corona is heated. We can avoid many of these by supposing the source of coronal energy to be radioactive atoms ejected from the deep interior of the Sun. Before discussing this hypothesis further we will review briefly the evidence for a high temperature corona.

7. Several independent lines of experimental evidence suggest *prima facie* that the corona is at a much greater temperature than the photosphere. They may be summarized as follows:—

| *Observation* | *Temperature* | *Authority* |
|---|---|---|
| 1. Electron velocities | $1{\cdot}1 \times 10^6$ | Grotrian * |
| 2. High ionization | $10^5$ | |
| 3. Width of line 5303 A. | $2{\cdot}3 \times 10^6$ | Lyot † |
| 4. Observations of solar radiation in wave-length 150 cm. | $10^7$ | Pawsey ‡ |

*Notes.*—1. Grotrian discussing the corona spectrum of 1929 states that if the coronal light is due to scattering by electrons, the absence of Fraunhofer lines requires Doppler shifts indicating velocities of $7{\cdot}5 \times 10^8$ cm. per sec., corresponding to $1{\cdot}1 \times 10^6$ degrees.

2. In full thermodynamical equilibrium and with an electron population of $4.10^8$ cm.$^{-3}$, an element of ionization potential 300 volts is half-ionized at a temperature of $10^5$ degrees.

3. Lyot's result, as modified by Hunter.

4. It has been pointed out to us by Dr. D. F. Martyn that radiation of wave-length 150 cm. is totally reflected by an electron population of $5.10^8$ cm.$^{-3}$, so that the observed radiation must originate in the corona.

Now despite the fact that a corona hotter than the photosphere implies a reversal of the temperature gradient, there is no objection to the high temperature on thermodynamic grounds provided that the corona is optically thin. There is a very close analogy with the hot ionosphere in the Earth's atmosphere. There must, of course, be some source of heat, which must be a non-radiative source unless it comes from some body at a temperature still higher than that of the corona.

The implication of a reversal of temperature gradient between photosphere and corona may explain an observational fact which has seemed anomalous for a number of years, namely the density gradient in the chromosphere.§ The density gradient of *H* deduced by Pannekoek and Minnaert from their observations of the line $H\gamma$, and also

* *Z. Astrophys.*, **3**, 220, 1931.

† Hunter, *Nature*, **150**, 756, 1942.

‡ Private communication (see *Nature*, **157**, 158, 1946).

§ *Cf.* Dyson and Woolley, *Eclipses of the Sun and Moon*, Chapters XI and XII, Oxford, 1937.

values deduced by Mitchell and Miss Williams from *Fe* and $Ti^+$ at a height of 2000 km., correspond to a temperature of 18,000°. Again, according to Unsöld, the contours of the absorption lines $H_3$ and $K_3$ in the chromosphere can be explained only by assuming Doppler effect due to a mean velocity of 18·4 km./sec., which gives $T = 18{,}600°$. McCrea has supposed that turbulent motions in the chromosphere produce these high velocities: but if the corona has a temperature very much higher than the photosphere, the chromospheric temperature may well be intermediate. We can, in fact, adduce the chromospheric observations as evidence in support of Lyot's hot corona.

It may be noticed that the ionization requires a temperature of $10^5$ while other observations require an electron velocity temperature of $10^6$, which is in qualitative agreement with expectation. Collision processes tend to produce an ionization equilibrium characteristic of $10^6$ degrees, but radiative processes tend to produce an ionization equilibrium characteristic of 6000°. The resultant degree of ionization will of course be characteristic of a temperature somewhere between these two. We have in fact the reverse of the type of disequilibrium usually encountered (as for example in the ionosphere).

8. It has been suggested by Vand * that the source of heat in the corona is the gravitational energy of particles of atomic dimensions falling into the Sun. If heat from this source is supposed to ionize *Fe* to *Fe*XIV and exhibit the coronal lines, the incoming particles must be guided (by a magnetic field, presumably) to those regions which show the lines strongly. Now coronal streamers do tend to terminate in active solar areas, and one may suppose that falling particles will certainly be ionized (as the electron pressure is so low) and will tend to move along the lines of force in a magnetic field. The coronal streamers may lie along lines of force. Hence the disturbed areas may attract falling particles. However, the corona always exhibits polar plumes, which should mean, if this theory is correct, a concentration of falling particles around the solar poles, whereas the coronal lines are extremely weak at the poles. One may say in general that while solar agencies may direct incoming energy to one part of the Sun rather than to another, they cannot alter the total amount of energy coming into the Sun from outside. Hence if the total intensity in the coronal lines varies appreciably through the sunspot cycle, the excitation is not likely to have any connection with a mechanism such as Vand's. The observations are not yet sufficient to determine this point.

9. A modification of Saha's theory which avoids energy difficulties by avoiding the use of neutrons may be constructed. If the source of coronal heat is solar, the energy must be derived from a part of the Sun at a greater temperature than the corona, namely from the deep interior of the Sun. Moreover, the energy must be transmitted from interior to corona by some agent which has little effect on the outer layers of the Sun through which it must pass. We are led to the idea of a radioactive element. A great variety of radioactive elements, with a great range of half-lives, have been observed in nuclear transformations. They may be supposed to be present in the deep interior of the Sun, in which case any solar material transported from the deep interior to the surface will be radioactive. On this view disturbed areas on the solar surface are simply seats of radioactivity. Rays of range 10 cm. in air at N.T.P. would penetrate the chromosphere easily, and expose the corona (with a population of $10^8$ particles per c.c.) to nearly the same heating and ionizing intensity as would be experienced by the photosphere (population of order $10^{13}$ cm.$^{-3}$) and chromosphere (population of order $10^{11}$ cm.$^{-3}$). If the corona has far less power of radiating away the energy absorbed per atom from the radioactive source, it may reach an equilibrium temperature far above the photospheric temperature.

The objections to Saha's original theory are absent. The $\alpha$ and $\beta$ particles have no special effects on protons, whereas neutrons attack protons to form deuterons with a strong exothermic reaction. As uranium plays no part in this theory there is no difficulty over

* *Nature*, 151, 728, 1943.

the uranium concentration in the photosphere. Lastly it is much easier to account for supplies of radioactive elements with half-lives of order several weeks than to account for supplies of neutrons which have extremely short lives in hydrogen atmospheres. Indeed, the manner in which solar disturbance persists for one or two rotations of the Sun, even in the case of the M regions which exhibit no spot structure, appears to be a strong argument for the presence of some form of atomic activity on the solar surface with a half-life of order about one month.

*Note added in Proof.*—Since the above was written the authors have seen a paper by Alfvén (*Ark. Mat. Astr. Fys.*, **27 A**, No. 25, 1941) in which reasons for accepting the high temperature of the corona are put forward. Alfvén deduces a temperature distribution with a maximum value of about $10^6$ from Baumbach's electron populations, assuming the corona to be in hydrostatic equilibrium under no forces except solar gravity. Also since the paper was written, it has been pointed out to the authors by Dr. C. W. Allen that the amount of cosmic material swept up annually by the Sun is insufficient to admit Vand's theory of coronal heating.

*Commonwealth Observatory,*
*Mt. Stromlo, Canberra :*
1945 *December* 4.

# THE NUMBER OF GALAXIES PER UNIT VOLUME

*A. Fletcher*

(Received 1946 January 10)

*Summary*

Current estimates of the number of galaxies per unit volume require to be approximately doubled, owing to a mistake of statistical technique which appears to have been overlooked.

---

1. An important part is played in cosmological theory by the mean density of matter in the universe, say $\rho$ grm./cm.$^3$. If the average mass of the galaxies (not necessarily the mass of an "average" galaxy), with allowance if necessary for intergalactic matter, is $\mu$ times the Sun's mass, and the number of galaxies per cubic megaparsec can be regarded as a constant, $\nu$, we have $\rho = 6{\cdot}8 \times 10^{-41} \mu\nu$. Any present estimate of $\mu$ is liable to be in error by a factor of about 10, and the matter is not discussed here. The value of $\nu$, on the other hand, has appeared to be comparatively well determined; but on examining the literature available to me, at the desire of my colleague Dr. A. G. Walker, I have discovered that current estimates of $\nu$ require to be approximately doubled. The value of $\nu$ may be estimated reasonably well from counts of nebulæ up to middle distances, without using distances so large that the apparent magnitudes are seriously affected by red-shift and relativity complications. Thus the present paper deals with nebulæ supposed uniformly distributed in Euclidean space.

2. The error lies in the type of calculation set out in some detail by Hubble.* A statement by Shapley † is evidently based on the same technique. The assumption of uniform density makes the problem so elementary from the point of view of classical stellar statistics that the result which I obtain below could hardly be new. To search no further, I notice that it is implicit in a result obtained in passing by Eddington ‡ in discussing the distribution of the nebulæ. But since the same lamented author has quoted § estimates by Shapley † and Hubble ‖ (without demur, curiously), and has used them in tentatively fitting a Lemaître model to the actual universe, it can hardly be superfluous to call attention to the necessary correction. Eddington's procedure is ingenious and indirect; a direct proof is therefore given below.¶

3. Let us suppose that the galaxies are uniformly distributed in space at the rate of $n$ per cubic parsec ($n = \nu \times 10^{-18}$), and that the luminosity function is independent of position. Then it is known that, neglecting absorption of light in space, the number of galaxies

* E. Hubble, *The Realm of the Nebulæ*, p. 188, Oxford, 1936. See also *Ap. J.*, 84, 552; or *Contr. Mt. Wilson Obs.*, 557, 1936.

† H. Shapley, *Galaxies*, p. 189, Philadelphia, 1943.

‡ A. S. Eddington, *M.N.*, 97, 158, 1937.

§ A. S. Eddington, *M.N.*, 104, 203, 1944.

‖ E. Hubble, *Smithsonian Report*, 121, 1942. Hubble's round-figure statement that there are about $10^8$ nebulæ in a sphere of radius $5 \times 10^8$ light-years gives $\nu = 6{\cdot}6$; Eddington quotes it as though it gave $\nu = 10$, which fortunately is nearer the true value.

¶ In this note (added 1946 February 21) I adopt the suggestion of a referee, and point out that, with some algebra, the final equation giving $f(m)$ in section 4 may be derived from the algebraical relations resulting from Schwarzschild's density law and a Gaussian distribution of absolute magnitudes, by suppressing the variation of density with position. See K. Schwarzschild, *A.N.*, 190 (4557), 361–376, 1912; or A. S. Eddington, *Stellar Movements*, pp. 211–212 (London, 1914); or B. J. Bok, *The Distribution of the Stars in Space*, pp. 15–16 (Chicago Univ. Press, 1937).

brighter than apparent magnitude $m$ is given by

$$\log N = 0{\cdot}6(m - m_1),$$

where the density-gradient coefficient 0·6 corresponds to the uniform density assumption, and $m_1$ is the space-density parameter. (All logarithms are to base 10 unless the contrary is indicated.) The form of the result is independent of the form of the luminosity function. If the luminosity function is known, the space-density $n$ may be determined from $m_1$, which will be taken to refer to the whole sky (the corresponding parameter for one square degree is $m_1 + 7{\cdot}69$).

If all the galaxies had the same absolute magnitude $M_0$, those apparently brighter than $m$ would lie within a sphere of radius $r$ parsecs, where

$$5 \log r = m + 5 - M_0,$$

and $n$ would be given by $3N/4\pi r^3$, where $N$ and $r$ relate to any same $m$; in particular, taking $m = m_1$, $N = 1$, and defining $r_0$ by

$$5 \log r_0 = m_1 + 5 - M_0,$$

we have $n = n_0$, say, where

$$n_0 = 3/4\pi {r_0}^3.$$

If, however, the absolute magnitudes are distributed in normal (Gaussian) fashion about a known mean value $M_0$ with known dispersion (standard deviation) $\sigma$, consideration of all galaxies down to a definite apparent magnitude favours intrinsically bright galaxies and causes the mean absolute magnitude $M_1$ of the galaxies observed to be brighter than $M_0$. (It is convenient in this paper to use the notation $M_1$ rather than the usual $\bar{M}$.) Hubble quotes from Malmquist * the result that the galaxies of any given apparent magnitude will have their absolute magnitudes distributed, also normally and with dispersion $\sigma$, about a mean value $M_1$, where

$$M_1 = M_0 - 1{\cdot}382\sigma^2,$$

the numerical factor being 0·6 $\log_e$ 10. This result may easily be verified to be correct. It has become customary to use $M_1$ instead of $M_0$ in various cases in which selection by apparent magnitude is involved; in particular, to calculate the space-density from

$$5 \log r_1 = m_1 + 5 - M_1,$$

$$n_1 = 3/4\pi {r_1}^3.$$

This is the process used by Hubble and others. In some circumstances the replacement of $M_0$ by $M_1$ is a proper correction for dispersion in the absolute magnitudes. But "$M_0 - 1{\cdot}382\sigma^2$" is not a panacea for all such troubles. *We shall prove that the mean absolute magnitude required in calculating the space-density is not* $M_1$, *but*

$$M_2 = \tfrac{1}{2}(M_0 + M_1) = M_0 - 0{\cdot}691\sigma^2.$$

4. The distribution of the galaxies in $(M, r)$ is supposed given by

$$dN = \frac{n}{\sqrt{2\pi}.\sigma} e^{-(M - M_0)^2/2\sigma^2} dM \,.\, 4\pi r^2 dr.$$

Since $M = m + 5 - 5 \log r$, we have $\partial(M, r)/\partial(m, r) = 1$, and the distribution in $(m, r)$ is

$$dN = \frac{\sqrt{8\pi}.n}{\sigma} r^2 e^{-(m + 5 - 5 \log r - M_0)^2/2\sigma^2} dm dr.$$

Thus the number with apparent magnitude between $m$ and $m + dm$ is $f(m)dm$, where

$$f(m) = \frac{\sqrt{8\pi}.n}{\sigma} \int_0^\infty r^2 e^{-(m + 5 - 5 \log r - M_0)^2/2\sigma^2} dr.$$

* K. G. Malmquist, *Ark. Mat. Astr. Fys.*, **16**, No. 23, 1922.

Putting $x = m + 5 - 5 \log r - M_0$ and $l = \log_e 10$, we have

$$f(m) = \frac{\sqrt{8\pi}.nl}{5\sigma} 10^{3(m+5-M_0)/5} \int_{-\infty}^{\infty} e^{-\frac{x^2}{2\sigma^2} - \frac{3lx}{5}} dx.$$

The value of the last integral is $\sqrt{2\pi}.\sigma e^{9l^2\sigma^2/50}$, or $\sqrt{2\pi}.\sigma.10^{9l\sigma^2/50}$, so that

$$f(m) = 10^{9l\sigma^2/50} \times \frac{4\pi nl}{5} 10^{3(m+5-M_0)/5}.$$

Thus the number of galaxies apparently brighter than $m$ is

$$N = \int_{-\infty}^{m} f(m)dm = 10^{9l\sigma^2/50} \times \frac{4\pi n}{3} 10^{3(m+5-M_0)/5},$$

so that

$$\log N = 0{\cdot}6(m - m_1),$$

where

$$m_1 = M_0 - 5 - \frac{5}{3} \log \frac{4\pi n}{3} - 0{\cdot}3l\sigma^2.$$

Thus, putting

$$M_2 = M_0 - 0{\cdot}3l\sigma^2 = M_0 - 0{\cdot}691\sigma^2 = \tfrac{1}{2}(M_0 + M_1)$$

and

$$5 \log r_2 = m_1 + 5 - M_2,$$

we have

$$n = 3/4\pi r_2^3, \qquad = n_2, \text{ say,}$$

which proves the result.

Thus the space-density $n_1$ deduced in the customary way by allowing one galaxy in the volume of a sphere of radius $r_1$ is no better and no worse than the totally uncorrected density $n_0$ corresponding to one galaxy per sphere of radius $r_0$. Both values are in error, $n_0$ above and $n_1$ below, by the same factor

$$e^{9l^2\sigma^2/50} = 10^{9l\sigma^2/50} = 10^{0{\cdot}4145\sigma^2},$$

which agrees with the factor $e^{b^2/4h^2}$ found by Eddington in 1937 on putting $b = 3l/5$ for uniform density and $2h^2 = 1/\sigma^2$. The true density is one galaxy per sphere of radius $r_2$, or $n = n_2 = \sqrt{n_0 n_1}$. With the assumptions made (density function constant, absolute magnitudes distributed normally and independently of position), the result is exact.

5. The effect of the correction on current estimates is sufficiently indicated by the following calculation, which claims no numerical finality. The observed magnitudes are in the region of

$$m_1 = 7{\cdot}48 \quad \text{(corresponding to 15·17 for one square degree),}$$

$$M_0 = -14{\cdot}2, \qquad \sigma = 0{\cdot}85,$$

from which

$$n_0 = 23{\cdot}4 \times 10^{-18}, \qquad M_1 = -15{\cdot}20, \qquad n_1 = 5{\cdot}9 \times 10^{-18}.$$

The proper calculation gives

$$M_2 = -14{\cdot}70, \qquad n_2 = 11{\cdot}7 \times 10^{-18}, \qquad n_2/n_1 = n_0/n_2 = 2{\cdot}0.$$

Thus the number of galaxies per cubic megaparsec is about 12 rather than about 6.

*Department of Applied Mathematics,*
*University of Liverpool:*
1946 *January* 8.

# ON A PROBLEM IN NAVIGATION

*W. M. Smart*

(Received 1946 January 4)

*Summary*

When the distance between the points F (latitude $\phi_1$, longitude $\lambda_1$) and T ($\phi_2$, $\lambda_2$) on a rhumb line is considerable, the departure between these points is related to the difference in longitude by the formula

$$\text{Departure} = (\lambda_2 - \lambda_1) \cos l;$$

$l$, called the "middle latitude", is given in terms of the mean latitude $\frac{1}{2}(\phi_1 + \phi_2)$ by

$$l = \tfrac{1}{2}(\phi_1 + \phi_2) + c,$$

in which $c$ is, in general, a comparatively small calculable angle depending on the co-ordinates of F and T. When the Earth is regarded as a sphere, the method of deriving $l$, or $c$, is well known. The question has recently been raised as to the general formula for $l$, or $c$, when the spheroidal nature of the Earth is taken into account; this note is intended to supply an answer.

---

1. One of the everyday problems of navigation may be stated as follows: given the latitude $\phi_1$ and longitude $\lambda_1$ of the point of departure F, and the distance steamed on a constant course, what are the co-ordinates ($\phi_2$, $\lambda_2$) of the point of arrival T? When the distance concerned is comparatively small—of the order of a hundred nautical miles, say—the information required can be easily found with all needful accuracy either by means of a mercator chart or by calculation from the following formulæ:—

$$\phi_2 - \phi_1 = \text{Distance} \times \cos C, \tag{1}$$

$$\text{Departure} = \text{Distance} \times \sin C, \tag{2}$$

$$\lambda_2 - \lambda_1 = \text{Departure} \times \sec \tfrac{1}{2}(\phi_1 + \phi_2), \tag{3}$$

in which (i) $C$ denotes the course-angle (the acute angle between the ship's rhumb line track and the north or south direction), (ii) distance and departure are measured in nautical miles, and (iii) the numerical values of $\phi_2 - \phi_1$ and $\lambda_2 - \lambda_1$ are expressed in minutes of arc in accordance with the usual definition of the nautical mile. Formulæ (1) and (2) combine to give

$$\tan C = \text{Departure}/(\phi_2 - \phi_1). \tag{4}$$

It is to be noted that (1) and (2)—and (4)—are accurate formulæ; on the other hand (3) is an approximate formula, although in the circumstances considered the error resulting from its use is negligible in practice.

The equations (1) to (4) can also be used, in the same circumstances, for calculating the distance and course-angle when the co-ordinates of F and T are given.

2. When, however, the distance between F and T is considerable—of the order of a thousand nautical miles or more—the formula (3) can no longer be used if accurate results are to be achieved. In this case the procedure involves the use of the "meridional parts" of the latitudes $\phi_1$ and $\phi_2$—we denote these by $M_1$ and $M_2$. If the Earth is regarded as a sphere, $M$ is defined by

$$M = 7915{\cdot}7 \log_{10} \tan\left(\frac{\pi}{4} + \frac{\phi}{2}\right), \tag{5}$$

the unit being 1′ of the longitude scale; this formula results from the fact that the mercator chart is a conformal representation of the Earth's surface. Translated into chart-measurements, $M$ is simply the distance of the parallel of latitude $\phi$ from the equator—both on the chart—in terms of the unit given by 1′ of longitude on the chart. The relation between $C$, $\lambda_1$, $\lambda_2$ and $M_1$, $M_2$ is then, accurately,

$$\lambda_2 - \lambda_1 = (M_2 - M_1) \tan C. \qquad (6)$$

In practice the value of $M_2 - M_1$ is obtained from a table of the function $M$ in (5), such as is found for example in Inman's collection of nautical tables.

In calculating $\phi_2$ and $\lambda_2$ when $C$, the distance steamed, and the co-ordinates $(\phi_1, \lambda_1)$ of F are given, we use (1) and (2), as before, together with a variant of (3) expressed in the form

$$\lambda_2 - \lambda_1 = \text{Departure} \times \sec l, \qquad (7)$$

where $l$ is referred to as the "middle latitude", its value being close to the mean latitude; we write $l$ in the form

$$l = \tfrac{1}{2}(\phi_1 + \phi_2) + c, \qquad (8)$$

in which we refer to $c$ as the "correction to the mean latitude".

For any given positions of F and T the corresponding value of $l$ can be readily derived, for, from (4), (6) and (7), we have

$$\cos l = (\phi_2 - \phi_1)/(M_2 - M_1). \qquad (9)$$

The corresponding value of $c$ can then be deduced. The values of $c$ derived in this way are tabulated in J. Inman, *Nautical Tables*, 114, 1942.

3. So far we have considered the Earth to be a sphere. But in problems of precision the spheroidal shape of the Earth must be taken into account. What must then be the formula corresponding to (9) which gives the correct value of $c$ in (8)?

We consider the meridians to be ellipses of eccentricity $e$; the equatorial radius is $a$, and this is the semi-major axis of the ellipse.

The ellipticity, $(a-b)/a$, of a meridian, where $b$ is the semi-minor axis, is 1/297; the value of $e^2$ is then given by

$$e^2 = 0{\cdot}0067227. \qquad (10)$$

In the figure, which shows part of the spheroid, let A and B be two neighbouring

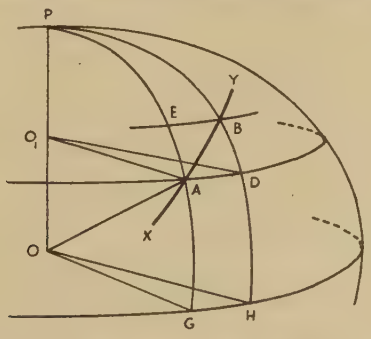


points on the rhumb line XY making an acute angle C with the meridians; let the *astronomical* latitudes of A and B be $\phi$ and $\phi + d\phi$ respectively. AD and EB are arcs of the parallels of latitude intercepted between the meridians PAG and PBH, the longitudes of these being $\lambda$ and $\lambda + d\lambda$. Then

$$\text{angle EAB} = \text{angle ABD} = C,$$

and

$$\text{angle AO}_1\text{D} = \text{angle GOH} = d\lambda,$$

where O and $O_1$ are respectively the centre of the spheroid and of the parallel of latitude through A.

We require the formulæ for $R$ (the radius of curvature of the meridian at A) and $R_1$ (the radius $O_1A$ of the parallel of latitude through A); these are given by

$$R = \frac{a(1-e^2)}{(1-e^2\sin^2\phi)^{3/2}} \tag{11}$$

and

$$R_1 = \frac{a\cos\phi}{(1-e^2\sin^2\phi)^{1/2}}. \tag{12}$$

Then

$$\mathrm{AE} = \mathrm{DB} = Rd\phi \tag{13}$$

and

$$\mathrm{AD} = R_1 d\lambda. \tag{14}$$

Since $\mathrm{AD} = \mathrm{DB}\tan C$, we have

$$R_1 d\lambda = Rd\phi \tan C, \tag{15}$$

from which

$$\lambda_2 - \lambda_1 = N(1-e^2)\tan C\int_{\phi_1}^{\phi_2} \frac{\sec\phi d\phi}{1-e^2\sin^2\phi}, \tag{16}$$

in which $(\lambda_2 - \lambda_1)$ is now expressed in minutes of arc and $N$ is the number of minutes of arc in a radian.

But, if $M$ denotes the meridional part for a place in astronomical latitude $\phi$, then

$$\lambda_2 - \lambda_1 = (M_2 - M_1)\tan C. \tag{17}$$

It follows from (16) and (17) that the function $M$ is given by

$$M = N(1-e^2)\int_0^{\phi} \frac{\sec\phi d\phi}{1-e^2\sin^2\phi}. \tag{18}$$

We shall show in section 5 how the values of $M$ can be derived from the tables of meridional parts *for a spherical earth*. Meanwhile, we assume that $M_1$ and $M_2$ in (17) are known.

4. Consider now the departure between F and T. The element of departure between A and B is AD or $Rd\phi\tan C$—from (14) and (15). The departure between F and T is then given by

$$\text{Departure} = \tan C\int_{\phi_1}^{\phi_2} Rd\phi. \tag{19}$$

If $l$ denotes the "middle latitude" for F and T, $l$ is defined by

$$\text{Departure} = (\lambda_2 - \lambda_1)\cos l, \tag{20}$$

the unit being the nautical mile corresponding to 1′ on the equator. In terms of $a$,

$$\text{Departure} = \frac{a}{N}(\lambda_2 - \lambda_1)\cos l \tag{21}$$

and from (17), (19) and (21) we obtain

$$a\cos l = \frac{N}{M_2 - M_1}\int_{\phi_1}^{\phi_2} Rd\phi.$$

Expanding $R$, given by (11), up to terms in $e^4$ and integrating, we find that

$$\cos l = \frac{N}{M_2 - M_1}[p\phi + q\sin 2\phi + r\sin 4\phi]_{\phi_1}^{\phi_2} \tag{22}$$

where

$$p = 1 - \tfrac{1}{4}e^2 - \tfrac{3}{64}e^4, \qquad q = -\tfrac{3}{8}e^2(1 + \tfrac{1}{4}e^2), \qquad r = \tfrac{15}{256}e^4.$$

If $\phi$ is expressed in minutes of arc, then, with the value of $e^2$ given in (10), we obtain

$$\cos l = \frac{1}{M_2 - M_1}[P\phi + Q \sin 2\phi + R \sin 4\phi]_{\phi_1}^{\phi_2}$$

where

$$P = p = 1 - 0{\cdot}0016828,$$
$$Q = Nq = -8{\cdot}683,$$
$$R = Nr = 0{\cdot}0091.$$

It is clear that we can safely ignore the term in $R$. Then we have finally

$$\cos l = \frac{\phi_2 - \phi_1}{M_2 - M_1}\left\{1 - 0{\cdot}0016828 - \frac{8{\cdot}683}{\phi_2 - \phi_1}(\sin 2\phi_2 - \sin 2\phi_1)\right\}. \tag{23}$$

This is the accurate formula for determining $l$ when the spheroidal shape of the Earth is taken into account.

The values of $c$—the correction to the mean astronomical latitude, given by $c = l - \frac{1}{2}(\phi_1 + \phi_2)$—can then be calculated for various latitudes and, for the sake of accuracy, should replace those tabulated in the case when the Earth is regarded as a sphere.

5. In this section we show how the meridional part $M$, used in the previous section, can be derived easily from the function given by (5) in the case of the spherical Earth.

Denote by $\theta$ the *geocentric* latitude corresponding to the astronomical latitude $\phi$; we have the well-known equation—

$$\tan \theta = (1 - e^2) \tan \phi. \tag{24}$$

The "angle of the vertical" is $\phi - \theta$ and its values are found in collections of tables; hence knowing $\phi$ we can easily find $\theta$.

In (18) $M$ is given as a function of $\phi$; we use (24) to transform it into a function of $\theta$. The result is easily seen to be

$$M = N\int_0^{\theta} \frac{\sec\theta(1 - 2e^2\cos^2\theta + e^4\cos^2\theta)^{\frac{1}{2}}}{1 - e^2\cos^2\theta}\,d\theta.$$

Expanding the integrand up to terms in $e^4$ and then integrating, we find that

$$M = N \log_e \tan\left(\frac{\pi}{4} + \frac{\theta}{2}\right) + \tfrac{1}{6}e^4 N \sin^3\theta,$$

or

$$M = 7915{\cdot}7 \log_{10} \tan\left(\frac{\pi}{4} + \frac{\theta}{2}\right) + 0{\cdot}026 \sin^3\theta. \tag{25}$$

The final term in this formula can be neglected.

Accordingly, the value of $M$ for the value $\phi$ of the astronomical latitude can be found from the tabulated values of $M$ for a spherical earth by *entering the tables with the corresponding geocentric latitude.*

*University Observatory,*
*Glasgow, W. 2.*
1946 *January* 3.

# THE CONTINUOUS RADIATIVE ABSORPTION CROSS-SECTION OF $O^-$

*D. R. Bates*

(Communicated by H. S. W. Massey)

(Received 1946 February 23)

In a study of the properties of the negative ions of oxygen, Bates and Massey * calculated the continuous radiative absorption cross-section of $O^-$. When this work was done the main application was thought to be in connection with the Earth's upper atmosphere, and consequently the published data were confined to the comparatively low

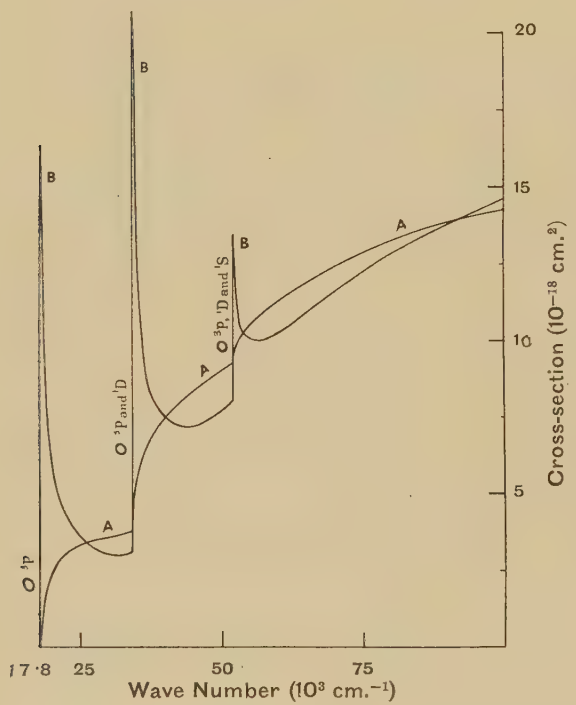


FIG. 1.—*Absorption cross-section of $O^-$ assuming detachment energy to be 2·2 e. volts.*
*Curve A—Polarizability parameter taken as 5·7 A.*
*Curve B—Polarizability parameter taken as 18·3 A.*

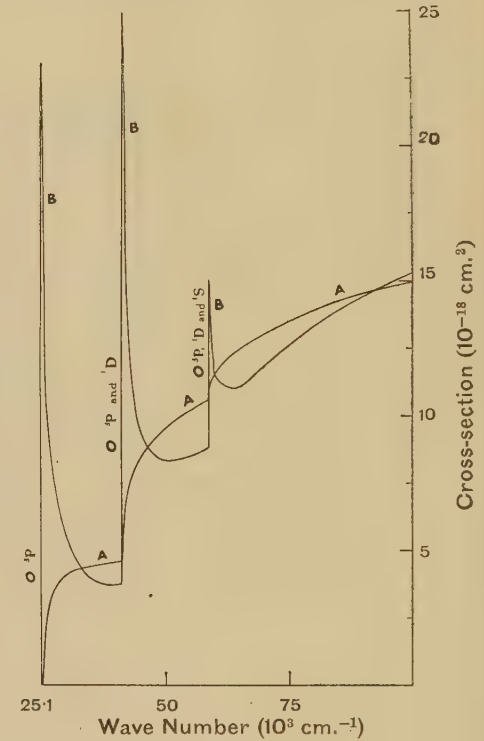


FIG. 2.—*Absorption cross-section of $O^-$ assuming detachment energy to be 3·1 e. volts.*
*Curve A—Polarizability parameter taken as 5·7 A.*
*Curve B—Polarizability parameter taken as 18·3 A.*

frequencies which are important in determining the total rate of photo detachment of electrons there.† Recently, however, Aller ‡ and Wildt and Chandrasekhar § have pointed out that the results may also be of value in discussing late-type stellar atmospheres.

* D. R. Bates and H. S. W. Massey, *Phil. Trans. Roy. Soc.*, A, 239, 269, 1943.
† D. R. Bates and H. S. W. Massey, *Proc. Roy. Soc.*, A, 187, 261, 1946.
‡ Private communication to Professor Massey.
§ R. Wildt and S. Chandrasekhar, *Ap. J.*, 100, 87, 1944.

In view of this and of other possible astrophysical applications, it is perhaps of interest to make generally available cross-section curves extended to higher frequencies (the computations for which had been carried out at the time of the earlier investigation).

The mathematical details will be found in the original paper and only results will be given here. Unfortunately, owing to various uncertainties, it is necessary to show several alternative cross-section curves:

(1) Two different values have been proposed for the electron affinity of $O$, 2·2 e. volts by Lozier * from collision experiments, and 3·1 e. volts by Vier and Mayer † from measurement of the equilibrium constant of the action,

$$O + e \rightleftharpoons O^-.$$

A decision cannot at present be arrived at as to which of these is correct. While general considerations tend to favour the former ‡, the astrophysical evidence put forward by Wildt and Chandrasekhar § tends to favour the latter. Results for both are therefore depicted (Figs. 1 and 2 respectively).

(2) The knowledge of the field in which the ejected electron moves is far from precise. To allow for this Bates and Massey || introduced a variable polarizability parameter. If the predicted value of this (5·7 atomic units) be taken the cross-section curves A are obtained. However, the possibility cannot be ignored (though it is felt to be improbable) that the effective polarizability may actually be so large (17·6 atomic units) that it brings about an additional node in the free $s$-wave function. This would cause what may be regarded as a resonance effect, the cross-section at the low frequency limit behaving as $\epsilon^{-\frac{1}{2}}$ instead of (as normally) $\epsilon^{+\frac{1}{2}}$ ($\epsilon$ being the excess energy of the incident photons). To illustrate the phenomena, curves B, which are calculated with a polarizability (18·3 atomic units) slightly above the critical value, are given.

It will be noted that the cross-section though very great at the limit does not tend to infinity—which only happens at *exact* resonance. Wildt and Chandrasekhar § erroneously criticized Bates and Massey || on this point.

*University College,*
*London:*
1946 *February* 21.

* W. Lozier, *Phys. Rev.*, 46, 268, 1934.
† D. T. Vier and J. E. Mayer, *J. chem. Phys.*, 12, 28, 1944.
‡ D. R. Bates, *Proc. Roy. Irish Acad.* In course of publication, 1946.
§ R. Wildt and S. Chandrasekhar, *Ap. J.*, 100, 87, 1944.
|| D. R. Bates and H. S. W. Massey, *Phil. Trans. Roy. Soc.*, A, 239, 269, 1943.

# SOME OBSERVATIONS OF THE H AND K LINES IN THE SOLAR SPECTRUM DURING A MAGNETIC STORM

*H. A. Brück and F. Rutllant*

(Received 1946 April 12)

*Summary*

An account is given of some photometric observations of the region near the H and K lines in the solar spectrum. One of the plates was taken on 1946 February 7 shortly after the commencement of a violent magnetic storm. An attempt is made to detect possible spectroscopic effects of the moving cloud of particles coming from the Sun. Profiles are derived for both the H and K lines, and slight indications are found of the existence of a small depression in the violet wings of both H and K on the critical date which would represent a velocity of the cloud of particles of some 750 km./sec.

---

1. *Introduction.*—On 1946 January 29 a group of unusually large sunspots appeared on the eastern limb of the Sun. On February 1 its total area, corrected for foreshortening, amounted to 4900 millionths of the Sun's hemisphere.* At Greenwich several solar flares were observed near the spot-group, at least three of which were of intensity 3 and five of which were followed by fade-outs. On February 5 the spot-group passed the central meridian of the Sun. Two days later a great magnetic storm, with ranges of the magnetic elements of 1°·3 in declination, more than 500 $\gamma$ in horizontal and nearly 400 $\gamma$ in vertical force, was recorded at Abinger as beginning abruptly at $10^h\ 20^m$ U.T. on February 7 and lasting for about 36 hours.†

The appearance of this group of spots suggested a search for possible spectroscopic effects of the earthwards moving cloud of particles which, being responsible for the magnetic storm, should also produce, according to Chapman ‡, a faint absorption on the violet side of the Fraunhofer lines. The actual existence of small effects of this kind has been reported recently from the Mount Wilson Observatory as having been observed by Richardson during the magnetic storms of 1941 September 18 and 1942 March 1.§

2. *The Observations.*—Photographs of the solar spectrum were obtained with the 21-foot Rowland concave grating of the Solar Physics Observatory, Cambridge, using the centre of a solar image of about 8 cm. in diameter. The grating was used in the first order, where it gives a dispersion of 2·56 A./mm., and the region of the H and K lines was chosen for the observations as promising in the present case the maximum chance of detection of the effect in question.

The photometric standardization of the plates was carried out with a Hilger step-wedge of rhodium sputtered on quartz. The transmissions of its six steps vary between 100 and 16 per cent. On account of the astigmatism peculiar to the concave grating, the step-wedge was placed about 1·85 m. in front of the spectrograph slit in accordance

* Cf. *Nature*, **157**, 155, 1946.

† Cf. *Nature*, **157**, 187, 1946.

‡ *M.N.*, **89**, 456, 1929.

§ Cf. *Annual Report Mount Wilson Observatory for 1943–44*, and *Trans. Amer. geophys. Un.*, **1944**, 558, 1945. The authors have great pleasure in expressing their thanks to Dr. Richardson, who kindly placed at their disposal some additional information on his observations.

with Sirk's * well-known construction for the horizontal image line. The solar image was formed on the step-wedge, and a cylindrical lens was introduced to re-focus the beam on to the slit of the spectrograph. Ilford Process plates were used with exposure times of the order of 4 minutes.

Altogether eight plates were secured in the interval between February 5 and 20, several of these through clouds and under poor general conditions. Four of the plates were measured in detail, but only three of them are of the same high quality showing excellent definition and practically the same optimum density in the spectral region concerned. Fortunately two of these three plates refer to dates which are of particular interest in connection with the magnetic storm observed at about the same time. This fact may perhaps lend some interest to their reduction, though for the detailed study of the present problem a considerably larger number of plates would be required. Details of the four plates used in this reduction are given in Table I.

TABLE I

*Plates*

| Plate | Date 1946 | U.T. h | m | Remarks |
|---|---|---|---|---|
| A | Feb. 5 | 12 | 40 | Spot on central meridian. Flare of intensity 2 between $11^h\ 35^m$ and $12^h\ 5^m$ and fade-out. |
| B | 7 | 12 | 51 | Magnetic storm begins at $10^h\ 20^m$. |
| C | 9 | 12 | 40 | Flare of intensity 3 between $11^h\ 50^m$ and $12^h\ 27^m$ and fade-out. |
| D | 20 | 10 | 30 | ... |

Photographic densities of these spectra were recorded with the Cambridge microphotometer using enlargements of 50 : 1 for the tracings. Three independent sets of records were made of the region near the H and K lines for each of the four plates, and electrometer deflections were measured in each tracing at 49 and 61 equidistant points, half an angstrom apart, for H and K respectively. The measured points cover a range of 12 and 15 A. on both sides of the line centres. The various sets of tracings were measured by the two observers independently, and though the abundance of blends in the wings of H and K made the drawing of the corresponding profiles difficult in some parts, good agreement was revealed when the two independent sets of measures were compared. Differences between the readings recorded by the two observers exceeded rarely 2 per cent. of the total deflections. For the reduction individual measurements were combined to means.

The measured deflections were converted in the usual manner into relative intensities. The characteristic curves were found to be closely similar in the case of all four plates. As the effect to be studied here should consist in small variations of the symmetry of the H and K profiles between the various dates, points of nearly the same intensity will have to be compared in the red and violet wings of each particular profile. Possible errors in the characteristic curves will therefore have only a secondary effect on the final results compared with the systematic and accidental errors connected with the drawing of the profiles on the tracings and their measurement. For similar reasons no attempt has been made to allow for the influence of limited resolving power and light scattered in the spectrograph.†

The results of the present observations are summarized in Tables II and III, of which the former gives the mean profile of the H and K lines, using plates A, B and D only, with the corresponding residuals. All intensities are expressed in percentages of the continuous spectrum near the lines the position of which was determined with the help of Minnaert's *Photometric Atlas of the Solar Spectrum.*

* *Astronomy and Astrophysics*, 13, 763, 1894.

† Central intensities in Table I are higher therefore than, for instance, in Thackeray's measurements (*M.N.*, 95, 293, 1935).

The behaviour of the residuals in Table II reveals the existence of real or apparent systematic differences between the profiles of the H and K lines on plates A, B and D. Their red wings, given by the figures in columns R, can be assumed to be uninfluenced by the effect which is to be examined in the present paper, and the size of the R residuals shows with what accuracy this equality is represented by our observations. Residuals for plate C, if included, would be nearly twice as large as for plates A, B and D, and since plate C being somewhat under-exposed is definitely inferior in quality to plates A, B and D, no data for C have been included in Tables II and III. It is noted, however, that the general run of the residuals for C follows that of the residuals in the case of plate D.

TABLE II

(a) *Profile of H*

| Distance from Centre | Mean Intensities (per cent.) Plates A, B, D | | Residual Intensities (per cent.) Plate A | | Plate B | | Plate D | |
|---|---|---|---|---|---|---|---|---|
| | R | V | R | V | R | V | R | V |
| A. | | | | | | | | |
| 0·0 | 13·3 | | +2·7 | | −1·3 | | −1·3 | |
| 0·5 | 16·5 | 16·5 | +3·0 | +3·0 | −1·5 | −1·5 | −1·5 | −1·5 |
| 1·0 | 19·2 | 19·5 | +2·8 | +2·5 | −1·2 | −1·0 | −1·7 | −1·5 |
| 1·5 | 23·5 | 23·5 | +2·0 | +2·0 | −0·5 | −0·5 | −1·5 | −1·5 |
| 2·0 | 27·8 | 27·8 | +1·7 | +1·7 | −0·3 | −0·3 | −1·3 | −1·3 |
| 2·5 | 32·3 | 32·7 | +1·2 | +0·8 | +0·2 | +0·3 | −1·3 | −1·2 |
| 3·0 | 37·3 | 38·2 | +1·2 | +0·8 | +0·7 | +0·3 | −1·8 | −1·2 |
| 3·5 | 43·0 | 43·7 | +1·0 | +0·3 | +0·5 | +0·3 | −1·5 | −0·7 |
| 4·0 | 48·7 | 49·2 | +0·3 | −0·2 | +0·3 | +0·3 | −0·7 | −0·2 |
| 4·5 | 54·0 | 54·5 | +0·5 | −0·5 | +0·5 | +0·5 | −1·0 | 0·0 |
| 5·0 | 60·3 | 60·2 | +0·7 | +0·8 | −0·3 | −0·7 | −0·3 | −0·2 |
| 5·5 | 65·7 | 65·2 | +1·3 | +0·8 | −0·7 | −0·7 | −0·7 | −0·2 |
| 6·0 | 70·7 | 69·0 | +1·3 | +1·0 | −0·7 | −1·0 | −0·7 | 0·0 |
| 6·5 | 76·7 | 73·3 | +1·3 | +0·7 | −1·2 | −1·3 | −0·2 | +0·7 |
| 7·0 | 81·7 | 77·7 | +1·3 | +0·8 | −1·7 | −1·2 | +0·3 | +0·3 |
| 7·5 | 85·0 | 81·0 | +1·0 | 0·0 | −1·0 | −2·0 | 0·0 | +2·0 |
| 8·0 | 87·5 | 82·5 | +1·5 | +0·5 | −1·0 | −1·0 | −0·5 | +0·5 |
| 8·5 | 89·3 | 85·8 | +1·7 | +1·5 | +0·2 | −1·5 | −1·8 | 0·0 |
| 9·0 | 91·7 | 87·7 | +2·3 | +1·8 | −0·7 | −1·2 | −1·7 | −0·7 |
| 9·5 | 93·8 | 88·8 | +2·2 | +2·2 | +0·2 | −1·3 | −2·3 | −0·8 |
| 10·0 | 95·8 | 89·3 | +1·7 | +2·7 | +1·2 | −1·8 | −2·8 | −0·8 |
| 10·5 | 97·0 | 91·0 | +1·5 | +2·0 | +1·5 | 0·0 | −3·0 | −2·0 |
| 11·0 | 97·7 | 91·7 | +0·8 | +2·3 | +1·8 | −0·7 | −2·7 | −1·7 |
| 11·5 | 98·3 | 93·3 | +1·2 | +1·7 | +1·2 | −1·3 | −2·3 | −0·3 |
| 12·0 | 98·7 | 93·3 | +1·3 | +1·7 | +1·3 | −1·3 | −2·7 | −0·3 |

The effect of the moving cloud of solar particles if present should be revealed by systematic differences between the violet wings of the different plates as given in columns V. It should appear in particular in the case of plate B, this being the plate which was taken shortly after the commencement of the magnetic storm. Here intensities V in the violet wing should be rather below normal. According to Table II this appears to be actually the case for a wave-length region beyond a distance of about 8 angstroms from the line centres of both H and K. However, on plate B both the red and violet wings of these lines appear to have been measured systematically below the average in the same wave-length region. For a test of the effect in question, intensity differences between the red and violet wings (R − V) will have to be considered. Values of these are given separately in Table III.

Unlike the intensities themselves these intensity differences should be practically independent of any systematic errors introduced into the shapes of the line profiles by errors in the characteristic curves of the plates.

Looking at Table III, the intensity differences in the cores of the two lines appear to be definitely smaller than the mean errors of measurement which according to the residuals in Table II are of the order of ±1 per cent. This is largely on account of the small

TABLE II

(b) *Profile of K*

| Distance from Centre | Mean Intensities (per cent.) Plates A, B, D | | Residual Intensities (per cent.) Plate A | | Plate B | | Plate D | |
|---|---|---|---|---|---|---|---|---|
| | R | V | R | V | R | V | R | V |
| A. | | | | | | | | |
| 0·0 | 11·7 | | +0·8 | | −0·7 | | −0·2 | |
| 0·5 | 13·8 | 14·0 | +0·7 | +0·5 | −0·3 | −0·5 | −0·3 | 0·0 |
| 1·0 | 16·2 | 16·2 | +0·8 | +0·3 | −0·2 | −0·2 | −0·7 | −0·2 |
| 1·5 | 18·5 | 18·7 | +1·0 | +0·8 | 0·0 | −0·2 | −1·0 | −0·7 |
| 2·0 | 21·3 | 21·3 | +0·7 | +0·7 | +0·2 | +0·2 | −0·8 | −0·8 |
| 2·5 | 24·0 | 24·0 | +0·5 | +0·5 | +0·5 | +0·0 | −1·0 | −0·5 |
| 3·0 | 27·3 | 27·0 | +0·2 | +0·5 | +0·7 | 0·0 | −0·8 | −0·5 |
| 3·5 | 31·0 | 30·3 | 0·0 | +0·7 | +1·0 | +0·2 | −1·0 | −0·8 |
| 4·0 | 34·7 | 33·8 | +0·3 | +0·7 | +1·3 | +0·2 | −1·7 | −0·8 |
| 4·5 | 38·3 | 37·3 | +0·2 | +0·7 | +0·7 | +0·2 | −0·8 | −0·8 |
| 5·0 | 42·3 | 41·5 | +0·7 | +0·5 | +0·2 | +0·5 | −0·8 | −1·0 |
| 5·5 | 47·7 | 46·2 | +0·3 | +1·3 | −0·7 | +0·3 | +0·3 | −1·7 |
| 6·0 | 52·2 | 50·8 | +0·8 | +0·7 | −1·2 | +0·2 | +0·3 | −0·8 |
| 6·5 | 57·2 | 56·0 | −0·7 | 0·0 | −1·2 | 0·0 | +1·8 | 0·0 |
| 7·0 | 61·7 | 59·7 | +0·3 | +0·3 | −1·7 | −0·2 | +1·3 | −0·2 |
| 7·5 | 65·8 | 64·0 | +0·2 | 0·0 | −1·8 | 0·0 | +1·8 | 0·0 |
| 8·0 | 69·2 | 67·7 | −0·2 | −0·7 | −1·2 | −0·2 | +1·3 | +0·8 |
| 8·5 | 72·5 | 70·7 | −0·5 | −0·7 | −1·5 | −1·2 | +2·0 | +1·8 |
| 9·0 | 75·5 | 73·5 | −0·5 | −0·5 | −1·5 | −2·5 | +2·0 | +3·0 |
| 9·5 | 77·8 | 75·8 | +0·2 | +0·2 | −1·3 | −2·8 | +1·2 | +2·7 |
| 10·0 | 80·2 | 78·0 | +0·8 | 0·0 | −1·2 | −2·5 | +0·3 | +2·5 |
| 10·5 | 82·0 | 79·7 | +1·0 | +0·3 | −1·0 | −2·7 | 0·0 | +2·3 |
| 11·0 | 83·2 | 81·0 | +0·8 | 0·0 | −0·7 | −2·0 | −0·2 | +2·0 |
| 11·5 | 84·5 | 82·8 | +1·0 | +0·2 | −0·5 | −1·3 | −0·5 | +1·2 |
| 12·0 | 85·8 | 84·5 | +0·2 | 0·0 | −0·3 | −0·5 | +0·2 | +0·5 |
| 12·5 | 87·2 | 85·5 | +0·3 | 0·0 | −0·2 | −0·5 | −0·2 | +0·5 |
| 13·0 | 88·2 | 86·5 | +0·3 | −0·5 | −0·2 | 0·0 | −0·2 | +0·5 |
| 13·5 | 88·5 | 87·8 | +1·0 | −0·3 | −0·5 | +0·2 | −0·5 | +0·2 |
| 14·0 | 88·8 | 88·2 | +0·7 | +0·3 | −0·8 | −0·2 | +0·2 | −0·2 |
| 14·5 | 90·0 | 88·5 | +1·0 | 0·0 | 0·0 | −0·5 | −1·0 | +0·5 |
| 15·0 | 91·0 | 89·5 | +1·0 | 0·0 | 0·0 | −0·5 | −1·0 | +0·5 |

influence which at this density variations in the readings of the photometer tracings, as registered by the two observers, have on the corresponding values of the intensities. The contrary is true for the outermost parts of the line wings as far as they have been measured here. In their case greater deviations between the different plates do not necessarily mean real differences since small variations in the measured readings of the original tracings produce relatively large effects on the intensities.

Assuming that plates A and D represent the "normal" profiles of the H and K lines, no systematic differences are found between these "normal" profiles and the one given by plate B in the region extending from 3 to about 9 angstroms away from the centres of

the lines. This at least is true as long as the H and K lines are considered both together. In the region near 10 angstroms small systematic differences between the R – V values of plate B and those of plates A and D appear to be indicated. This would correspond to a depression of the violet wings of both H and K of about a little over one per cent. between a distance of roughly 9 to 11 angstroms from the line centres, which would mean an

TABLE III

*Intensity Differences (R – V) between the Red and Violet Wings of H and K (per cent.)*

| Distance from Centre | H Plates | | | K Plates | | | Distance from Centre |
|---|---|---|---|---|---|---|---|
| | A | B | D | A | B | D | |
| A. | | | | | | | A. |
| 0·5 | 0·0 | 0·0 | 0·0 | +0·2 | +0·2 | −0·3 | 0·5 |
| 1·0 | +0·3 | −0·2 | −0·2 | +0·5 | 0·0 | −0·5 | 1·0 |
| 1·5 | 0·0 | 0·0 | 0·0 | +0·2 | +0·2 | −0·3 | 1·5 |
| 2·0 | 0·0 | 0·0 | 0·0 | 0·0 | 0·0 | 0·0 | 2·0 |
| 2·5 | +0·4 | −0·1 | −0·1 | 0·0 | +0·5 | −0·5 | 2·5 |
| 3·0 | +0·4 | +0·4 | −0·6 | −0·3 | +0·7 | −0·3 | 3·0 |
| 3·5 | +0·7 | +0·2 | −0·8 | −0·7 | +0·8 | −0·2 | 3·5 |
| 4·0 | +0·5 | 0·0 | −0·5 | −0·4 | +1·1 | −0·9 | 4·0 |
| 4·5 | +1·0 | 0·0 | −1·0 | −0·5 | +0·5 | 0·0 | 4·5 |
| 5·0 | −0·1 | +0·4 | −0·1 | +0·2 | −0·3 | +0·2 | 5·0 |
| 5·5 | +0·5 | 0·0 | −0·5 | −1·0 | −1·0 | +2·0 | 5·5 |
| 6·0 | +0·3 | +0·3 | −0·7 | +0·1 | −1·4 | +1·1 | 6·0 |
| 6·5 | +0·6 | +0·1 | −0·9 | −0·7 | −1·2 | +1·8 | 6·5 |
| 7·0 | +0·5 | −0·5 | 0·0 | 0·0 | −1·5 | +1·5 | 7·0 |
| 7·5 | +1·0 | +1·0 | −2·0 | +0·2 | −1·8 | +1·8 | 7·5 |
| 8·0 | +1·0 | 0·0 | −1·0 | +0·5 | −1·0 | +0·5 | 8·0 |
| 8·5 | +0·2 | +1·7 | −1·8 | +0·2 | −0·3 | +0·2 | 8·5 |
| 9·0 | +0·5 | +0·5 | −1·0 | 0·0 | +1·0 | −1·0 | 9·0 |
| 9·5 | 0·0 | +1·5 | −1·5 | 0·0 | +1·5 | −1·5 | 9·5 |
| 10·0 | −1·0 | +3·0 | −2·0 | +0·8 | +1·3 | −2·3 | 10·0 |
| 10·5 | −0·5 | +1·5 | −1·0 | +0·7 | +1·7 | −2·3 | 10·5 |
| 11·0 | −1·5 | +2·5 | −1·0 | +0·8 | +1·3 | −2·2 | 11·0 |
| 11·5 | −0·5 | +2·5 | −2·0 | +0·8 | +1·2 | −1·7 | 11·5 |
| 12·0 | −0·4 | +2·6 | −2·4 | +0·2 | +0·2 | −0·3 | 12·0 |
| 12·5 | | | | +0·3 | +0·3 | −0·7 | 12·5 |
| 13·0 | | | | +0·8 | −0·2 | −0·7 | 13·0 |
| 13·5 | | | | +1·3 | −0·7 | −0·7 | 13·5 |
| 14·0 | | | | +0·4 | −0·6 | +0·4 | 14·0 |
| 14·5 | | | | +1·0 | +0·5 | −1·5 | 14·5 |
| 15·0 | | | | +1·0 | +0·5 | −1·5 | 15·0 |

average velocity of the moving cloud of particles of the order of 750 km./sec. The effect would still be present if plate C were added to the "normal" plates A and D. The behaviour of the K line on plate B in the region neighbouring 7 angstroms, which is not shared by the H line, should, however, show that further observations based on a considerably larger material of plates will be required before the reality of such an effect can be finally accepted. On the other hand the direction and the magnitude of the effect indicated by the present observations is in good agreement with the observations of Mount Wilson Observatory which have been mentioned previously.

*Observatory, Cambridge:*
1946 *April.*

# THE SPECTRUM OF T CORONÆ BOREALIS ON 1946 FEBRUARY 11

*C. C. L. Gregory and Eleanor M. Peachey*

(Received 1946 February 26)

Through thin cloud a spectrum of this star was obtained at U.T. $2^h\ 40^m$ on an Ilford Zenith plate with the 4-prism spectrograph attached to the Wilson 24-inch reflector, the time of exposure being 68 minutes. The general appearance of the spectrum is of nova type—broad emission lines accompanied by broad absorption lines on the side of shorter wave-length. The strongest lines are due to hydrogen and the next in strength to helium I. The plate was measured and reduced in the usual way, corrections being made for annual and diurnal motion and for curvature. Settings were made on the estimated centres of the lines and also on the edges of all the stronger lines. From these measures, converted to wave-lengths, were subtracted the adopted tabular wave-lengths of the lines of probable origin. The wave-length differences thus obtained were converted to velocities in km./sec. and are given in the table:

| 1 | 2 | 3 | 4 | 5 | 6 | 7 | 8 |
|---|---|---|---|---|---|---|---|
| Element | Adopted Tabular Wave-length | Emission Centre | Emission Width | Absorption Centre | Absorption Width | Violet Edge | Total Range of Velocity |
| | | km./sec. | km./sec. | km./sec. | km./sec. | km./sec. | km./sec. |
| Hydrogen | | | | | | | |
| *Hγ* | 4340·5 | +140 | 1180 | −1000 | 1100 | −1530 | 2360 |
| *Hδ* | 4101·8 | + 40 | 930 | − 890 | 1180 | −1530 | 2130 |
| *Hε* | 3970·1 | +180 | 1090 | − 950 | 1010 | −1530 | 2170 |
| *Hζ* | 3889·0 | + 40 | 870 | −1040 | 1110 | −1530 | 2030 |
| *Hη* | 3835·4 | +140 | ... | − 550 | ... | ... | ... |
| *He*I | 4471·5 | (−190) | (720) | −1000 | 970 | −1530 | (1720) |
| ,, | 4387·9 | − 30 | 880 | − 640 | 630 | −1010 | 1520 |
| ,, | 4143·8 | + 10 | ... | − 420 | ... | ... | ... |
| ,, | 4026·2 | +100 | 770 | − 780 | 760 | −1110 | 1560 |
| *C*II | 4267·2 | +140 | ... | ... | ... | ... | ... |
| *Fe*II | 4233·2 | +100 | 820 | − 580 | 920 | −1160 | 1770 |
| *Fe*II (blend of λ 4178·9 and λ 4173·5) | 4176·2 | + 90 | 680 | − 630 | 620 | − 940 | 1360 |
| *He*II | 4199·9 | (− 10) | ... | − 430 | ... | ... | ... |
| *Ca*II | 3933·7 | (+260) | 760 | − 630 | ... | ... | ... |

In column 1 are listed the elements giving rise to each line, and in column 2 the adopted tabular wave-lengths, a mean wave-length being adopted for the blend *Fe*II λ 4173 and λ 4179. In the case of the line at λ 4200, the wave-length adopted was that of *He*II λ 4199·9, but the line was probably a blend with *N*III λ 4200·0 and λ 4195·7. In the case of the line near λ 3934, the wave-length adopted was that of *Ca*II λ 3933·7, but a blend with *N*III λ 3938·5 and λ 3934·4 is suspected. Columns 3 and 5 give the recessional velocities obtained from measures of the centres of the emission and absorption lines respectively, and columns 4 and 6 give the widths in km./sec. of the emission and absorption lines respectively. The broad emission line due to *He*I λ 4471 appeared very faint, although the absorption was strong, and values relating to measures of its edges and centre are in brackets as doubtful, as are also the values in column 3 relating

to the lines identified as being due to *He*II and *Ca*II. Column 7 gives the recessional velocity obtained from measures of the extreme violet edges of the absorption lines; these negative values represent the maximum velocity of approach of the gases giving rise to the absorption. Column 8 gives the total range of velocity obtained by taking the differences between the measures of the extreme violet edges of the absorption lines and the extreme red edges of the emission lines.

It will be noted that the numbers in column 8 are somewhat greater than the sum of the corresponding numbers in columns 4 and 6, indicating a gap between the red edges of the absorption lines and the violet edges of the emission lines. The effect is probably not real but due to the finite width of the slit.

*University of London Observatory,*
*Mill Hill Park, N.W. 7:*
1946 *February* 25.

# THE SPECTRUM OF THE CORONA AT THE ECLIPSE OF 1940 OCTOBER 1

*C. W. Allen*

(Communicated by the Commonwealth Astronomer)

(Received 1946 January 16)

*Summary*

Three coronal spectra obtained at the eclipse of 1940 October 1 have been investigated. Wave-lengths and intensities of seven coronal emission lines are tabulated. The continuous spectrum is found to redden slightly as the solar distance increases. The intensities of absorption lines in the outer corona are measured to obtain $\mathcal{J}_F/\mathcal{J}_S$, the ratio of the intensity of Fraunhofer component of the spectrum to the total intensity. This ratio increases with increasing solar distances, but $\mathcal{J}_F$ decreases. $\mathcal{J}_F/\mathcal{J}_S$ is independent of wave-length. The red shift of the Fraunhofer lines is measured to be 0·08 A. ±0·04, but the reality of the shift is doubted. The observations are thought to confirm Grotrian's theory of the coronal continuous spectrum in general, but it is suggested that $\mathcal{J}_F$ is caused by diffraction instead of reflection by interplanetary particles. Theory of diffraction indicates a radius of particles $\rho = 10^{-3}$ cm., and density at the distance of the Earth $N_E = 3 \times 10^{-15}$ per c.c.

---

The Australian eclipse expedition to South Africa in 1940 was organised by the Commonwealth Observatory * for the purpose of obtaining new observations relating to the physics of the Earth's ionosphere and the solar corona. The ionospheric results and the observations of coronal polarization have been published †, and the present paper completes the report of the observational programme by describing the coronal spectra.

1. *Equipment.*—The spectrograph consisted of a 60° glass prism with a 6-inch edge and 4 inches in height, a 4-inch Zeiss camera lens with a focal length of 20 inches, and 4½-inch telescope collimator with a focal length of 64 inches. The spectrum was photographed on cinema film since the focus field was strongly curved and it was desired to obtain the whole visible spectrum in as sharp a focus as possible. The film was mounted on a ring of radius 9 cm. which could be rotated in steps. Seven spectra could be photographed on one piece of film. The spectrograph was covered by a small hut and the prism box was well enclosed with bricks to keep the temperature as steady as possible.

The spectrograph was fed by a 6-inch telescope of 80 inches focal length and an 8-inch cœlostat with no secondary mirror. All parts were mounted on brick piers. It was, of course, necessary to have the telescope and spectrograph oriented correctly long before the day of the eclipse. This was done in such a way that the image of the eclipsed Sun did not fall centrally on the slit but at one end of it with the east limb about 1 mm. within the length of the slit. The slit was vertical and radial to the Sun. At the time of the eclipse it was oriented 6° south of the Sun's eastern equator. Very small adjustments to the orientation of the cœlostat axis could have corrected any small error in the alignment of the spectrograph without appreciably affecting the drive.

A Hilger spectrograph slit 22 mm. long was used, and this was provided with small

* Previously "Commonwealth Solar Observatory".

† A. J. Higgs, *M.N.*, **102**, 24, 1942; C. W. Allen, *M.N.*, **101**, 281, 1941.

prisms at top and bottom for reflecting the wave-length comparison into the spectrograph. The comparison spectra were given by helium and mercury-argon discharge tubes run from a 6-volt battery and a small Ford coil. Care was taken to insure that the comparison spectrum beam filled the collimator from both top and bottom of the slit.

The film used was Eastman plus X 35 mm., developed with Kodak Fine-Grain developer for 18 min. at 65° F.

2. *Eclipse Photographs.*—Three coronal spectra were obtained during the 230 seconds of totality. Exposures were made for 10 seconds, 170 seconds, and 27 seconds, but for the 170-second exposure the inner part of the corona (to 0·4 of Sun's radius) was shaded off for 120 seconds. The three spectra are reproduced in Fig. 1 (see Plate 4). The wave-length comparison spectra were impressed during the eclipse. For the 10-second exposure there was time to obtain only the *He* comparison spectrum; for the remaining exposures both *He* and *Hg – A* comparison spectra were obtained.

The coronal spectra were satisfactory for photometry, but the Fraunhofer lines in the outer corona were not as strong as expected. The flash spectrum appeared near the limb in the first exposure (10 seconds) which commenced 5 seconds after second contact.

3. *Control Exposures and Photometry.*—Standardization of the densities of the film at all wave-lengths was obtained by exposing spectra through a step wedge. The wedge was calibrated by photographic photometry and was found to be substantially neutral. Some solar spectra for comparison with the Fraunhofer component of the coronal spectrum were obtained by using the illumination from shaded dark grey paper.

In order to obtain spectra with an intensity distribution similar to that of the Sun, some exposures were made of the illumination from sun-lit white blotting-paper. In this case reductions of slit width and aperture were necessary in order to secure suitable densities. These spectra were found to be considerably more intense in the blue relative to the red than the coronal spectra.

Wave-length control exposures could not be made in full daylight as the comparison line spectrum was then strongly superimposed with a Fraunhofer spectrum. This difficulty was overcome by taking some spectra of white paper in twilight and using a black background for the discharge tubes.

A complete set of microphotometer tracings was made with the photometer of the Radcliffe Observatory shortly after the eclipse. Intensity calibration curves were drawn from the step wedge tracings at wave-lengths 4000 A., 4500 A., 4800 A., 5400 A., and 6200 A. When plotted on a logarithmic intensity scale the group of curves for 4000 A., 4500 A., and 4800 A. were parallel, and the group for 5400 A. and 6200 A. were parallel. Average curves were obtained for each group. The red group was steeper, *i.e.* had greater contrast, than the violet group.

4. *Coronal Emission Lines.*—Seven of the well-known coronal emission lines were detected on our spectra, and measurements gave the following wave-lengths: 3801·2, 3987·2, 4086·2, 4230·8, 5115·8, 5302·9, and 6373·7 A.

The intensities of these lines were measured and expressed in equivalent breadths of the coronal continuous spectrum. In Fig. 2 the equivalent breadths are plotted against $R/s$, where $R$ is the projected distance from the Sun's centre, and $s$ the Sun's radius. The equivalent breadths at a distance of 3 minutes of arc from the Sun's limb (*i.e.* $R = 1{\cdot}2s$) are shown in Table I which contains also similar observations by Grotrian.* The differences in both the absolute and relative intensities of the lines support the view that the coronal lines are highly variable.

TABLE I

| Wave-length (A.) | 3801 | 3987 | 4086 | 4231 | 5116 | 5303 | 6374 |
|---|---|---|---|---|---|---|---|
| Equivalent breath (A.) | 0·2 | 0·2 | 0·1 | 0·5 | 0·5 | (10) | 3 |
| Grotrian's values (A.) | ... | 0·2 | 0·3 | 0·8 | 1·2 | 27·5 | 2·8 |

* W. Grotrian, *Z. Astrophys.*, 7, 26, 1933.

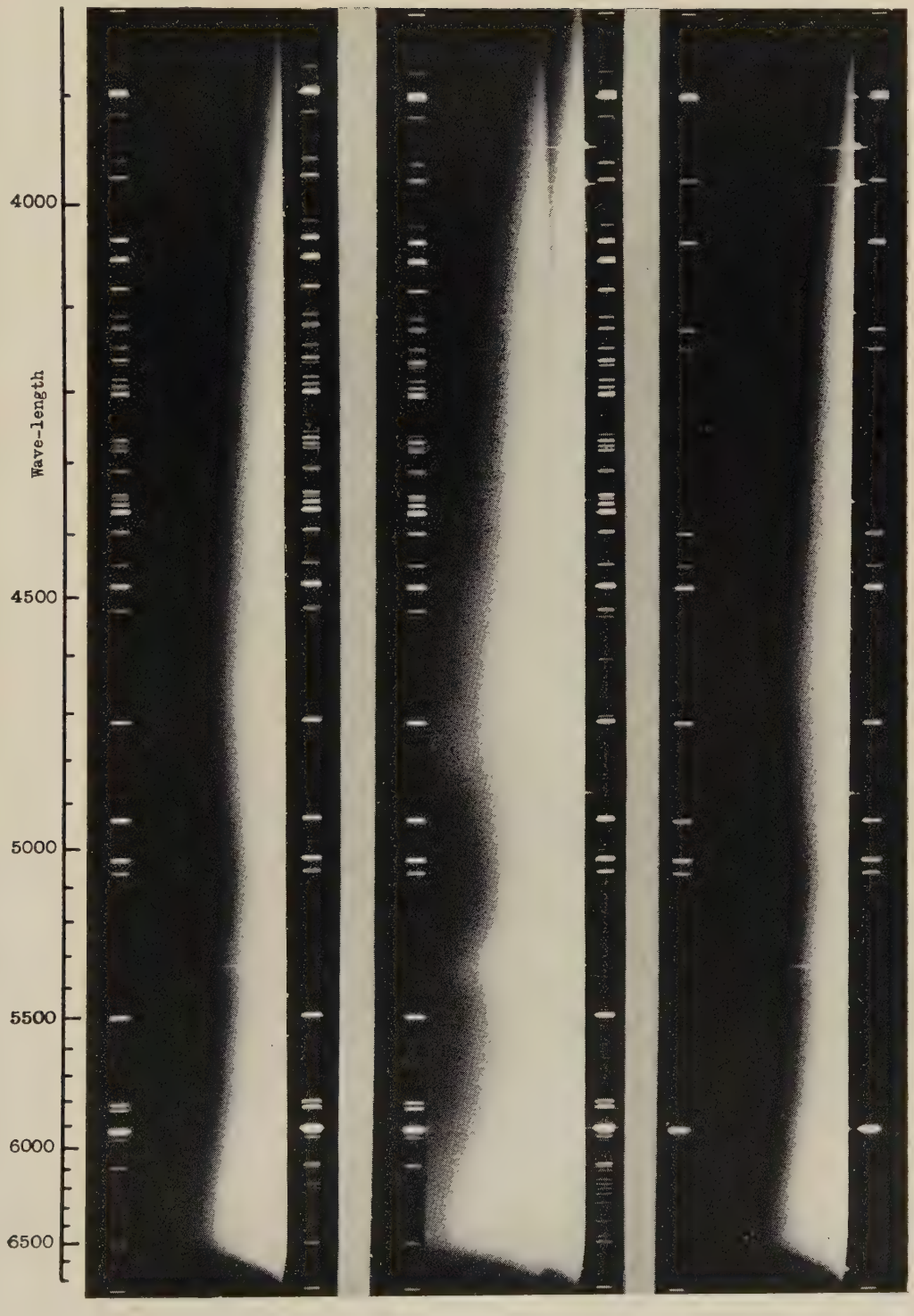


Fig. 1.—Coronal Spectra.
Exposures; (A) 27 secs. (B) 170 secs. (C) 10 secs. Enlarged ×4·6.

Fig. 2 shows that the equivalent breadth of all coronal emission lines decreases with height above the Sun's surface, but the rate of decrease is not the same for all lines. Grotrian (*loc. cit.*) has found that for certain coronal lines the equivalent breadth remains constant with distance from the Sun, but his observations refer mainly to smaller values of $R$ than those discussed here.

The observed breadth of the coronal lines is governed by the resolution of the spectrograph and of course shows no measurable variation with distance from the Sun.

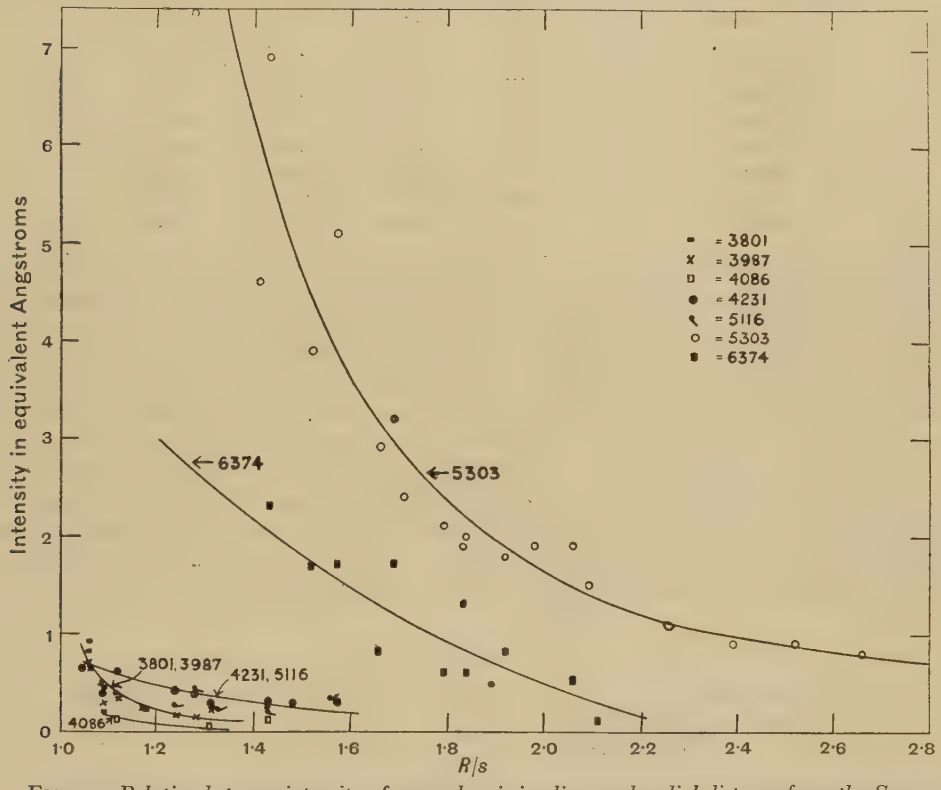


FIG. 2.—*Relation between intensity of coronal emission lines and radial distance from the Sun.*

5. *Continuous Spectrum.*—No provision was made for a careful comparison of the intensity distribution of the corona spectrum with that of the Sun. Spectra of white blotting-paper illuminated by direct sunlight were found to be much richer in violet light than the corona, but it is assumed that the difference was due to the colour of the paper, illumination from the blue sky, differential mirror reflection with colour, etc. The researches of Ludendorff* and Grotrian† have shown satisfactorily that the colour of the corona is the same as that of the Sun.

Microphotograms for solar distances varying from $R = 1{\cdot}2s$ to $R = 2{\cdot}6s$ show that the coronal radiation reddens slightly as the distance from the Sun is increased. The microphotograms for the 170-second exposures are reproduced in Fig. 3. The change of colour with $R$ may be expressed by comparing spectral intensity distributions with the distribution at a selected value of $R$, viz. $R = 1{\cdot}8s$. The intensities for various values of $R$ obtained by direct application of the intensity calibration curves were multiplied by appropriate factors to make all equal at 4200 A. The intensities then found relative to those at $R = 1{\cdot}8s$ are shown in Table II.

* H. Ludendorff, *S.B. Preuss. Akad. Wiss.*, 5, 83, 1925.

† W. Grotrian, *Z. Astrophys.*, 3, 199, 1931.

These figures give the distribution of intensity relative to the distribution at $R = 1{\cdot}8s$. It will be seen that the red end of the spectrum becomes about 20 per cent. or 30 per cent. more intense relative to the violet as $R$ is increased from $1{\cdot}2s$ to $2{\cdot}4s$.

TABLE II

*Intensity Distribution of the Coronal Spectrum at various Solar Radii relative to the Distribution at $R = 1{\cdot}8s$.*

| Wave-length | Mean $R =$ | $1{\cdot}2s$ | $1{\cdot}6s$ | $2{\cdot}0s$ | $2{\cdot}4s$ |
|---|---|---|---|---|---|
| 6500 A. | | 0·80 | 0·93 | 1·07 | 1·16 |
| 6300 | | ... | 0·96 | 1·04 | 1·03 |
| 5400 | | 0·95 | 0·98 | 1·02 | 0·96 |
| 5300 | | 0·95 | 0·97 | 1·02 | 0·98 |
| 4620 | | 0·97 | 0·99 | 1·00 | 0·94 |
| 4300 | | 0·98 | 1·00 | 1·00 | 1·02 |
| 4160 | | 1·02 | 1·00 | 0·99 | 0·99 |
| 4000 | | 1·02 | 1·01 | 0·99 | 0·99 |

This result was obtained by comparison of regions of the spectrum where photographic densities differed considerably, and the apparent change of colour might have been affected by errors in the photographic characteristic curves (see Section 3), especially by any error in the determined change of contrast with colour. For this reason the change of corona colour with $R$ was re-determined by comparing coronal spectra having approximately the same density but different values of $R$ as found on the three exposures. By combining the two short exposures (10 seconds and 27 seconds) and comparing these with the long exposure (170 seconds) it was found that densities were comparable when $R$ was about $0{\cdot}6s$ greater on the long than the short exposures. When intensities were reduced to the same value at 4200 A., as before, it was found that the intensity in the red was greater for the longer exposure, *i.e.* for the greater value of $R$. The result is shown in Table III. In this case there is an increase of 9 per cent. in reduced red intensity for a radial difference of $0{\cdot}6s$.

TABLE III

| Wave-length (A.) | | 4200 | 4600 | 5400 | 6300 |
|---|---|---|---|---|---|
| Reduced intensity | $\frac{\text{long exposure}}{\text{short exposure}}$ | 1·00 | 1·02 | 1·05 | 1·09 |

This is in reasonable agreement with the 20 per cent. or 30 per cent. difference found for the range $R = 1{\cdot}2s$ to $2{\cdot}4s$, *i.e.* a radial difference of $1{\cdot}2s$. Both methods of examining the data lead to a slight reddening of the coronal spectrum with increase of radial distance.

This result may be compared with those of Ludendorff (*loc. cit.*) and Grotrian * who found no change of colour with radial distance. However, Ludendorff's observations were limited to the region 3820 A. to 4840 A., while Grotrian's observations extended only to $R = 1{\cdot}35s$. The change of coronal colour with $R$, as demonstrated in Tables II and III, is hardly great enough to be revealed in a smaller range of either radial distance or wave-length.

The diminution of intensity with radial distance has been measured on the spectra and in the range $R = 1{\cdot}2s$ to $2{\cdot}6s$ is proportional to $R^{-6{\cdot}5}$. Photometric observations on the direct solar image at the same eclipse gave intensity proportional to $R^{-7{\cdot}0}$ in the same range of $R$. The spectroscopic measurements of course refer to only a single equatorial direction, whereas the photometry of the direct photographs was averaged for all directions.

If the continuous coronal spectrum is caused by scattered sunlight, Fraunhofer lines would appear throughout the corona unless these are enormously broadened by velocity displacements. Broadening up to 50 A. would not be enough to eliminate all evidence

* *Z. Astrophys.*, 3, 199, 1931.

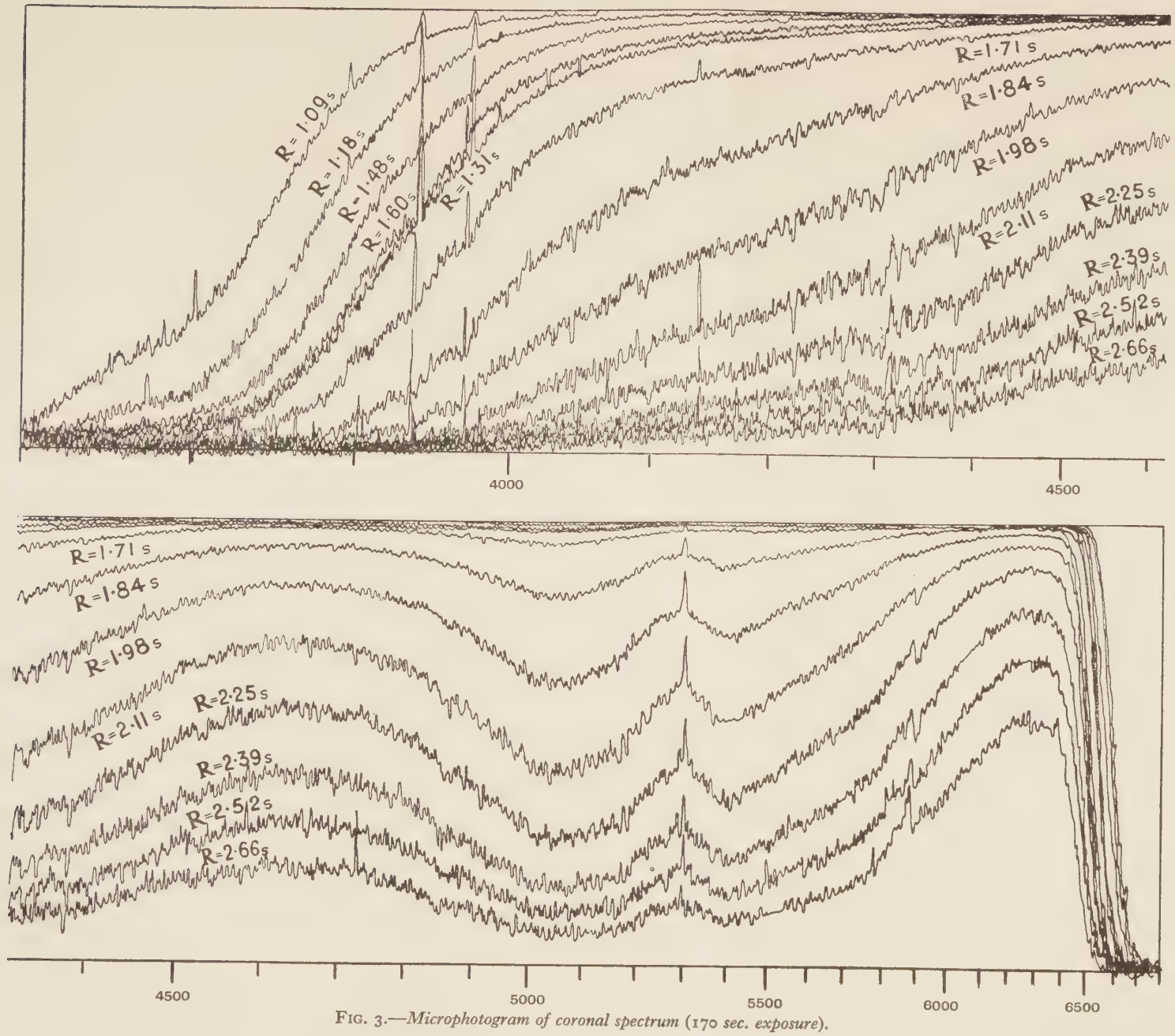


FIG. 3.—*Microphotogram of coronal spectrum* (170 *sec. exposure*).

[*Facing page* 140.

of strong groups of absorption lines. The microphotograms of continuous coronal spectra shown in Fig. 3, show no evidence of depressions in the neighbourhood of the heavy line concentrations of the solar spectrum, which occur at 3830 A., 3950 A., and 4290 A. However, very slight humps occurring at 4100 A. and 3750 A. in the continuous coronal spectra might mark the edge of depressions about 160 A. wide centred at the line concentrations. The depressions would then cover the regions 3750–3910 A., 3870–4030 A., 4210–4370 A., and might leave a hump at 3750 A. and from 4030–4210 A. Grotrian (*loc. cit.*) has concluded that his observed difference between the intensity of the coronal and the continuous solar spectrum is caused by a sinking of the coronal curve in the region of strong Fraunhofer lines. His diagram (Abb. 7) shows humps at about 4150 A. and 3700 A. in the coronal continuous intensity in agreement with the present results. As Grotrian has pointed out, if the continuous coronal spectrum is sunlight scattered by electrons their velocity must be of the order of 7500 km./sec., more than ten times greater than the thermal velocity.

6. *The Intensities of Absorption Lines in the Corona.*—As at earlier eclipses absorption lines have made their appearance in the outer portions of the corona. They can be seen in the microphotograms shown in Fig. 3. The wave-lengths and intensities are similar to a somewhat weakened Fraunhofer spectrum.

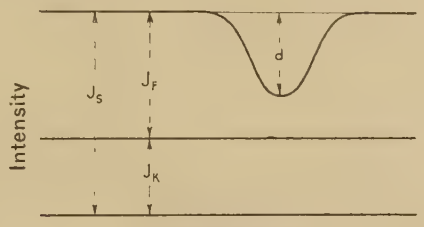


FIG. 4.

We now assume that the total intensity of the coronal spectrum $\mathcal{J}_S$ is made up of a Fraunhofer component $\mathcal{J}_F$, with Fraunhofer lines of solar intensity, and a purely continuous component $\mathcal{J}_K$ with no absorption lines. This is in agreement with Grotrian's theory of the corona* where $\mathcal{J}_F$ is the intensity of light scattered by particles, and $\mathcal{J}_K$ that scattered by electrons. Referring to the absorption line represented in Fig. 4, it will be seen that the usual measurement of depth of a Fraunhofer line in the solar spectrum would yield $d/\mathcal{J}_F$, while in the corona, where the continuous intensity $\mathcal{J}_K$ is superimposed, the depth measurement would yield $d/\mathcal{J}_S$. Consequently the ratio of the Fraunhofer line depths measured in the corona and the solar spectrum gives an estimate of $\mathcal{J}_F/\mathcal{J}_S$. This result would need modification if there were any difference in the observed breadth of lines in the Sun and the corona, but no such difference can be detected with the eclipse spectrograph (resolving power about 4000 at 4000 A.).

The depths of 27 lines or features have been measured from the tracings of both the solar and coronal spectra. The lines were distributed between 3934 A. and 5893 A., and could be detected in the coronal spectra from $R = 1{\cdot}28s$ to $2{\cdot}66s$. The observed depth ratios, giving $\mathcal{J}_F/\mathcal{J}_S$, are plotted against the solar radial distance in Fig. 5, which also contains Grotrian's observations.† The diagram gives the impression that $\mathcal{J}_F/\mathcal{J}_S$ approaches 1·0 in the more distant parts of the corona. It will be noticed that for smaller values of $R$ Grotrian's estimate of the intensity of the Fraunhofer component is two or three times greater than that of the author.

The variation of $\mathcal{J}_F$ with $R$ may be obtained by multiplying $\mathcal{J}_S$ by $\mathcal{J}_F/\mathcal{J}_S$. We have

* W. Grotrian, *Z. Astrophys.*, 8, 124, 1934; see Dyson and Woolley, *Eclipses of the Sun and Moon*, p. 155, Oxford, 1937.

† *Z. Astrophys.*, 8, 124, 1934.

already seen (Section 5) $\mathcal{J}_S$ to be proportional to $R^{-6\cdot5}$, and the variation found for $\mathcal{J}_F$ is shown in Fig. 6. The absolute value of $\mathcal{J}_F$ in terms of the brightness of the Sun's surface is found by using the law $\mathcal{J}_S \propto R^{-6\cdot5}$, integrating, and making the total brightness of the

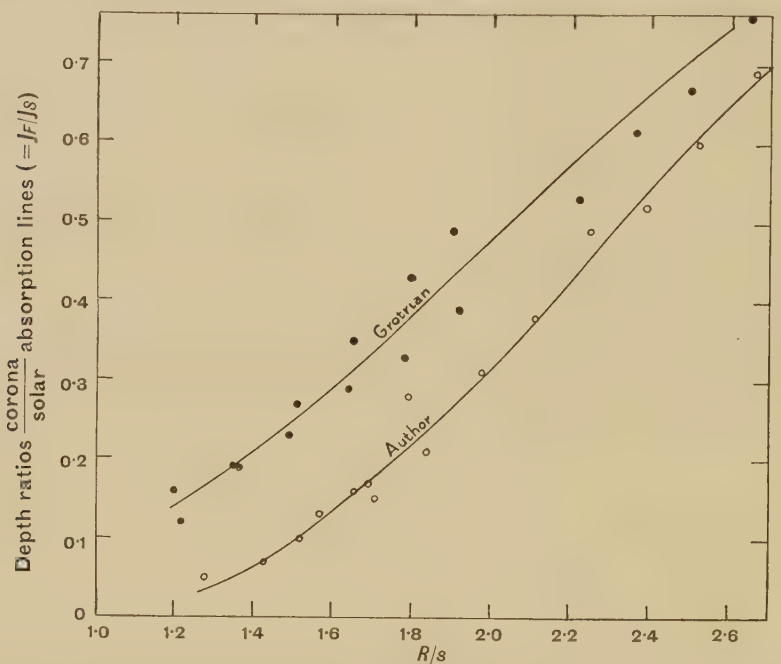


FIG. 5.—*Relation between the strength of the Fraunhofer lines and the radial distance from the Sun.*

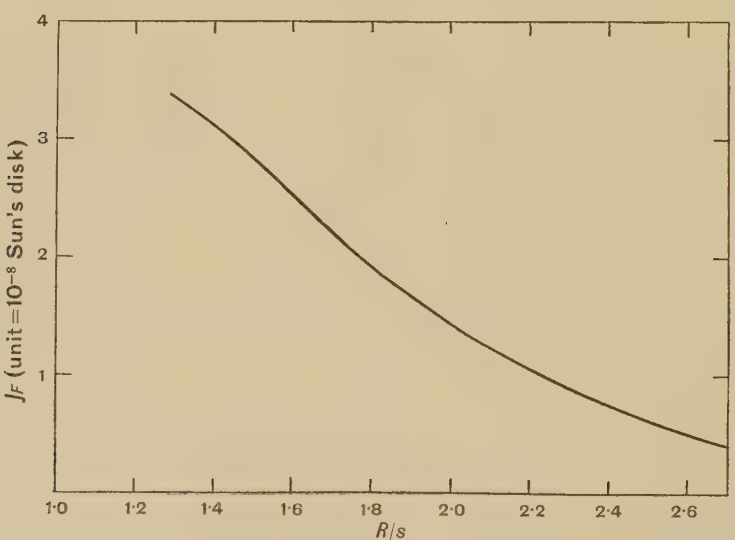


FIG. 6.—*Intensity variation of the Fraunhofer component of the corona radiation.*

corona $10^{-6}$ times that of the Sun. $\mathcal{J}_F/\mathcal{J}_S$ is taken from Fig. 5 and it has been assumed that the equatorial intensity is twice the mean intensity. The rapid decrease of $\mathcal{J}_F$ with increasing $R$ shows that the Fraunhofer lines in the corona do not come from scattering in the Earth's atmosphere or in the optical system. There would be no reason to expect such scattering to vary appreciably with $R$.

We next study the change of $\mathcal{J}_F/\mathcal{J}_S$ with wave-length. For this purpose at each radial distance the ratios of the coronal line depths to the solar line depths for individual lines were divided by the mean value for all lines at that radius. The ratios so obtained were averaged over varying $R$ for each spectrum line and the results are plotted against wave-length in Fig. 7. In spite of the scarcity of lines at the red end of the spectrum it is clear that there is no appreciable change of $\mathcal{J}_F/\mathcal{J}_S$ with wave-length. Thus the wave-length distribution of $\mathcal{J}_F$ is the same as $\mathcal{J}_S$, and hence the same as for the Sun. Since the accuracy of this result is obviously better than one power of the wave-length (see Fig. 7), the coronal Fraunhofer lines cannot be due to Rayleigh scattering of atoms which would make $\mathcal{J}_F/\mathcal{J}_S$ approximately proportional to $\lambda^{-4}$. The particles which scatter the Fraunhofer spectrum must be large compared with the wave-length of light. A theory which ascribes this Fraunhofer component to diffraction by interplanetary particles is given in Section 9.

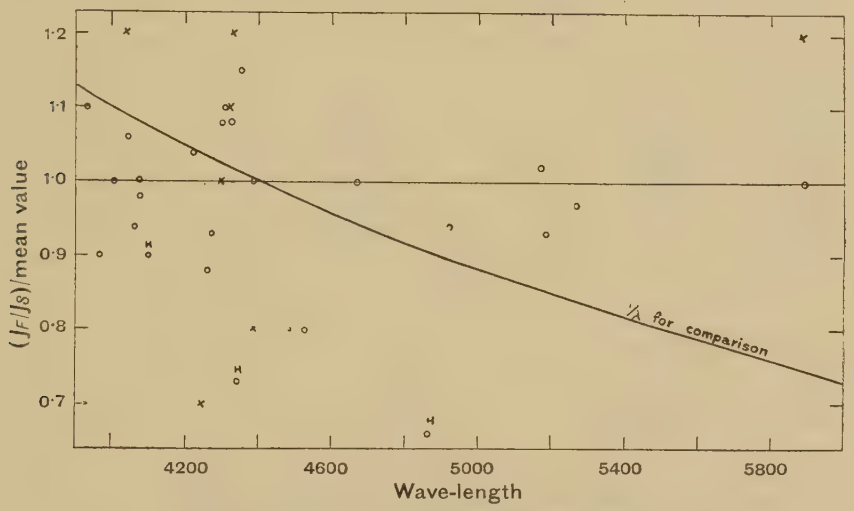


FIG. 7.—*Variation of* $\mathcal{J}_F/\mathcal{J}_S$ *with wave-length.*
O—*From* 170 *sec. exposure.*
X—*From* 10 *sec. and* 27 *sec. exposures.*
H—*Hydrogen lines.*

The hydrogen lines in Fig. 7 are marked H. The small values for these lines are undoubtedly due to traces of hydrogen emission from the flash spectrum. There was also evidence of emission of the *He* line 5875 A. throughout the whole of the corona.

7. *The Wave-length of Absorption Lines in the Corona.*—Careful measurements of the wave-lengths of the Fraunhofer lines visible in the outer corona have been made by comparison with the discharge tube spectra provided on either side of the coronal spectrum. The same Fraunhofer lines were also measured on the control solar spectra and the differences in the solar and coronal wave-lengths were tabulated for several sets of measurements by three observers. Unfortunately it was difficult to set accurately on the faint absorption lines. Some of the lines were found to be displaced to the red and others to the violet, and it seems probable that this inconsistency was due mainly to the difference in the appearance of the lines as seen strongly in the solar spectrum and weakly in the coronal spectrum. The measurements of both coronal and solar wave-lengths are shown in Table IV, from which a mean shift of $+0{\cdot}084 \pm 0{\cdot}04$ A. for the coronal lines relative to the solar lines is obtained. As the mean wave-length of the group of lines measured is 4200 A., the velocity implied is 6 km./sec. The measurements were made by three different observers, and, as can be seen in Table V, these observations showed a disconcerting disagreement.

It is quite evident from the tabulated measurements by different observers that the variations in the measured displacements do not satisfy the rules of random errors. The probable error quoted for the final displacement (±0·04 A.) is an approximate estimate based on Table IV and Table V. The red displacement of coronal lines is not much greater than the probable error and the reality of the shift could not be regarded as established by the present observations. The shift of 0·08 A. is much smaller than the 0·3 A. shift observed by Moore * although it is in the same direction. The present measurement casts some doubt on the reality of the red shift discovered by Moore and the existence of a red shift might be regarded as not yet finally settled.

TABLE IV

*Wave-lengths of Fraunhofer lines in the Corona and the Sun*

| Wave-lengths | | Displacement | Wt. | Wave-lengths | | Displacement | Wt. |
|---|---|---|---|---|---|---|---|
| Corona | Sun | | | Corona | Sun | | |
| 3998·06 | 3997·83 | +·23 | 71 | 4250·07 | 4250·38 | −·31 | 7 |
| 4005·41 | 4005·18 | +·23 | 26 | 4260·63 | 4260·30 | +·33 | 15 |
| 4041·15 | 4040·92 | +·23 | 17 | 4289·77 | 4289·88 | −·11 | 29 |
| 4045·73 | 4045·64 | +·09 | 94 | 4325·22 | 4324·92 | +·30 | 44 |
| 4063·71 | 4063·62 | +·09 | 41 | 4352·10 | 4351·75 | +·35 | 33 |
| 4071·40 | 4071·63 | −·23 | 47 | 4383·67 | 4383·72 | −·05 | 35 |
| 4101·26 | 4101·43 | −·17 | 8 | 4481·37 | 4481·05 | +·32 | 6 |
| 4226·64 | 4226·75 | −·11 | 56 | 4667·31 | 4667·14 | +·17 | 9 |

TABLE V

| Observer | Displacement | Weight |
|---|---|---|
| C. W. A. | +0·13 A. | 32 |
| S. C. B. G. | +0·06 A. | 16 |
| N. G. C. | −0·06 A. | 7 |
| Mean | +0·08 A. | |

8. *Discussion.*—The coronal observations of the 1940 eclipse give general support to the theory of the corona outlined by Grotrian (*loc. cit.*), who suggests that the sources of coronal light (other than emission lines) are (*a*) sunlight reflected by particles, and (*b*) sunlight scattered by electrons. The ratio of intensity of these two sources is given by $\mathcal{J}_F/\mathcal{J}_K$, which can readily be found from the observations of the depth of Fraunhofer lines (Section 6). The ratio has been found to be independent of wave-length and to increase with solar distance. The colour of light scattered from free electrons should be almost independent of solar distance † and hence the slight reddening of coronal light described in Section 5, if real, must imply that the light scattered from the particles is reddish. This, however, would result in an increase of $\mathcal{J}_F/\mathcal{J}_S$ as one approached the red, which is not observed in Fig. 7. Compromising on these two conclusions it may be decided that the particle scattering is either neutral or slightly reddish. There is certainly no evidence that it is blue, and we can reject Minnaert's suggestion that the Fraunhofer component may be due to Rayleigh scattering by atoms.

The degree of polarization as a function of $R$ is in reasonable agreement with Grotrian's theory provided experimental inaccuracy is taken into consideration. Minnaert has computed the theoretical polarization on the supposition that the corona is composed of perfectly polarizing material (*e.g.* electrons). His computations are plotted against the reciprocal of the radial distance in Fig. 8, where we have used a mean of "blue" and "yellow" polarization, and an $r^{-5}$ distribution of scattered light per c.c. Here $r$ is the radial distance from the centre of the Sun, and the $r^{-5}$ distribution is appropriate for our

* J. H. Moore, *P.A.S.P.*, 35, 333, 1923; 45, 147, 1933.
† M. Minnaert, *Z. Astrophys.*, 1, 209, 1930.

$R^{-6\cdot5}$ distribution of coronal intensity.* We have also added the curve which would be obtained if the Fraunhofer component $\mathcal{J}_F$ had no polarization. The author's mean polarization measurements for the same eclipse † are included in Fig. 8, and also the polarization measurements for the particular orientation of the spectrograph slit (6° south of eastern equator). It should be remarked that the measurements of both polarization and $\mathcal{J}_F$ may be seriously influenced by stray light for $s/R < 0\cdot5$. A correction for stray

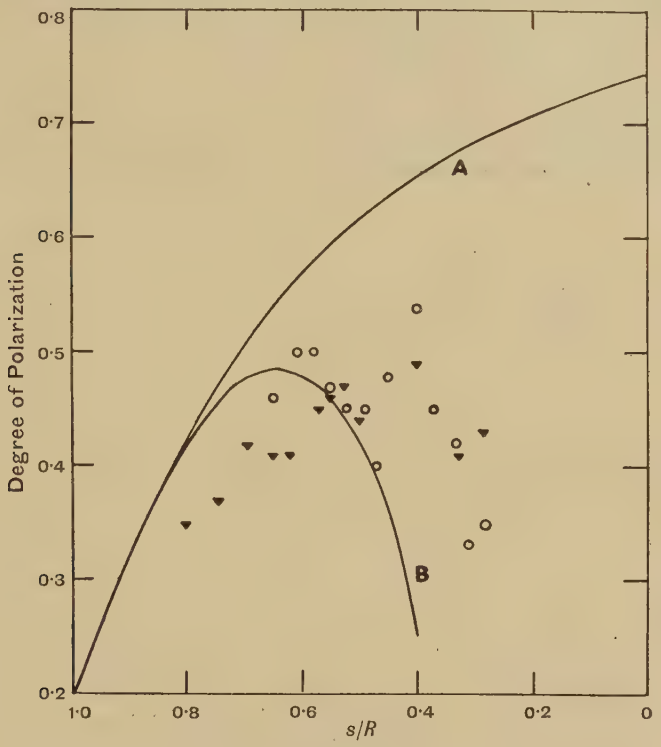


Fig. 8.—*Variation of corona polarization with distance from Sun.*
A—*Corona material polarizes completely.* B—$\mathcal{J}_F$ *not polarized.*
▼—*Mean polarization measurement.* o—*Oriented polarization measurement.*

light was applied in the case of the polarization measurements, but not for the measurements of $\mathcal{J}_F/\mathcal{J}_S$ which is used for determining $\mathcal{J}_F$. Furthermore, the existence of considerable polarization at large distances from the Sun has been judged by the visibility of the coronal streamers. The streamers must be associated with matter coming from the Sun—electrons on Grotrian's theory—and one would expect them to be strongly polarized. The particles contributing to $\mathcal{J}_F$ would form a structureless cloud and might be mistaken for stray light. If this is so the polarization measurements would be over-corrected and too high. Taking these points into consideration, the polarization observations are in sufficient agreement with the supposition that $\mathcal{J}_F$ is the unpolarized contribution of particles, and the remainder of the continuous spectrum due to polarized scattering by electrons.

The main difficulty of the Grotrian theory is that it demands an increasing concentration of scattering particles as one approaches the Sun. By comparing the intensity of the corona and the zodiacal light Grotrian finds a particle distribution of $r^{-1\cdot5}$, and to account for the observed increase of $\mathcal{J}_F$ with decreasing $R$ when $R < 1\cdot8s$ it is necessary to assume that the particle concentration continues to increase almost up to the Sun's surface. On

* Minnaert, *loc. cit.*, p. 219. † *M.N.*, 101, 281, 1941.

the other hand Russell * has shown that all small particles would vaporize within a finite radial distance. This radius we will assume to be $4s$, which from Russell's formula would correspond to a vaporizing temperature of 2025° K. One would not expect a very high concentration of particles just outside the radius where the particles are vaporized.

In order to overcome the above difficulty it is now suggested that the Fraunhofer lines visible in the outer corona are caused by *diffraction* by interplanetary particles. The increase of intensity of $\mathcal{J}_F$ as one approaches the Sun is then explained by the increase of intensity of light diffracted by small particles as the diffracting angle $\theta$ approaches zero.

9. *Diffraction by Interplanetary Particles.*—The diffraction of the Sun's light by small particles in the Earth's atmosphere has given a satisfactory explanation of the meteorological coronas produced by dust and water droplets, and the theory developed for atmospheric particles is now applied to interplanetary material.

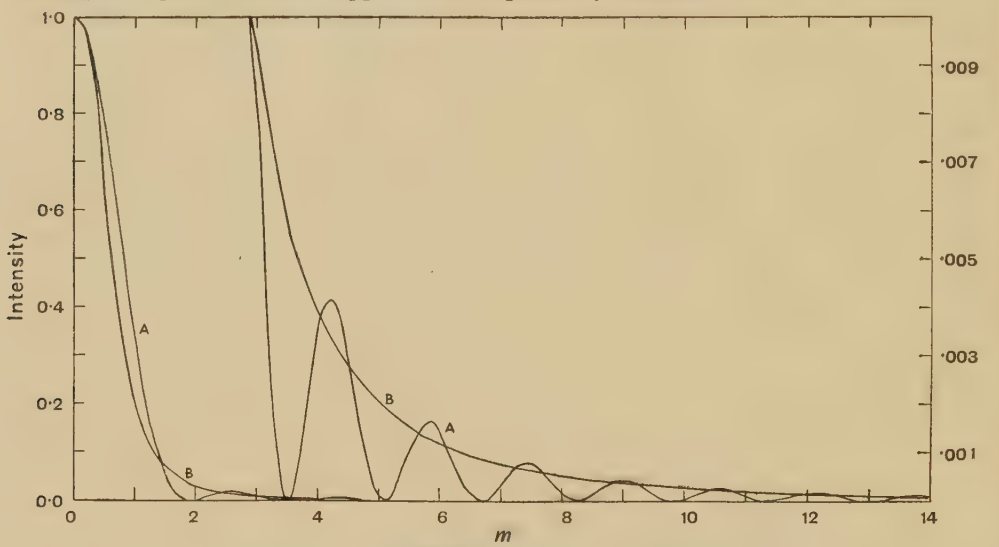


Fig. 9.—*Comparison of diffraction intensity curves.*
A—*Diffraction formula.*
B—*Intensity* $= 1/(1+4m^3)$.

The variation of intensity of diffracted light with $\theta$, the angle between the incident and the diffracted beam, has been calculated † in the terms of $m$, where $m = \pi\rho \sin\theta/\lambda$, $\rho$ = radius of the particles, and $\lambda$ = the wave-length of the radiation. The calculations have been made for circular openings in an opaque screen and Babinet's principle invoked to show that the diffraction by opaque disks of particles would be the same. The variation of diffracted intensity with $m$ is shown in Fig. 9. In order to overcome integration difficulties we have used the expression $1/(1+4m^3)$ instead of the tabulated values (Humphreys, *loc. cit.*) of the intensity. The two curves are compared in Fig. 9. As there is certain to be a good deal of variation in the diameter of the diffracting particles, the subsidiary maxima would be smoothed out in practice and the expression used should be a fair approximation.

In order to obtain the intensity of diffracted light it is necessary to determine the constant $K$ by which $1/(1+4m^3)$ should be multiplied. This may be done by equating the flux of radiation passing through one circular aperture to the integrated diffracted light, then

$$I\Omega\pi\rho^2 = \int_0^{2\pi}\int_0^{\infty} \frac{K\theta\, d\theta\, d\phi}{1+4\pi^3\rho^3\theta^3/\lambda^3} = \frac{4^{1/3}\lambda^2}{3\sqrt{3\rho^2}}K,$$

* H. N. Russell, *Ap. J.*, 69, 49, 1929.
† W. J. Humphreys, *Physics of the Air*, pp. 530–532, 1920. (Original table by Airy.)

where $I$ is the intensity of the light source, $\Omega$ the solid angle it subtends at the aperture, $\rho$ the radius of the aperture, $\lambda$ the wave-length, $\theta$ the angle between the incident and diffracted ray which is considered to be small, and $\phi$ the azimuthal co-ordinate.

Then

$$K = 10{\cdot}2\, I\Omega\rho^4/\lambda^2.$$

Hence the solar radiation diffracted per solid angle per c.c. containing $N$ circular apertures, or by Babinet's principle $N$ opaque disks of radius $\rho$, will be

$$10{\cdot}2\, I\Omega N \frac{\rho^4}{\lambda^2(1 + 4\pi^3\rho^3\theta^3/\lambda^3)},$$

where $I$ is now the intensity of the Sun's surface, and $\Omega$ the solid angle subtended by the Sun at the particles. The intensity $i$ of scattered light viewed from the Earth E (Fig. 10) will now be

$$i = 10{\cdot}2\frac{\rho^4 I}{\lambda^2}\int_0^\infty \frac{\pi s^2}{r^2} N \frac{dL}{1 + 4\pi^3\rho^3\theta^3/\lambda^3},$$

where $s$ is the Sun's radius, $r$ the radial distance of the particles from the Sun, and $L$ their distance from the Earth. With sufficient approximation for small $\theta$, where $dL = -dr$,

$$i = 10\, I\frac{\pi\rho^4 s^2}{\lambda^2}\int_D^{4S} \frac{N(r)r\,dr}{r^3 + 4\pi^3\rho^3 R^3/\lambda^3},$$

where $N$ is now a function of $r$, $D$ is the distance of the Earth from the Sun, $4s$ is the distance within which particles are volatilized, $R$ is the perpendicular distance of the Sun from the ray, and $R/r = \theta$.

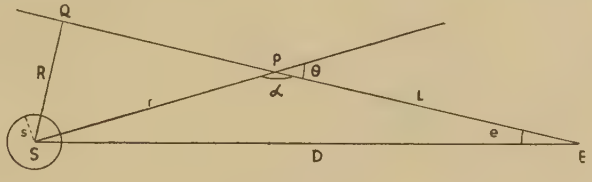


FIG. 10.

Evaluations of this integral were tabulated for

$$\rho = 10^{-4},\ 10^{-3},\ 10^{-2},\ 10^{-1},\text{ and } 1 \text{ cm.},$$
$$\lambda = 4300 \text{ A. and } 6300 \text{ A.},$$
$$R = 1{\cdot}0s,\ 1{\cdot}5s,\ 2{\cdot}0s,\ 2{\cdot}5s,\text{ and } 3{\cdot}0s,$$

and

$$N(r) = N_E, \qquad N(r) = N_E(D/r), \quad \text{and} \quad N(r) = N_E(D/r)^2.$$

Here $N_E$ is the number of particles per c.c. at the distance of the Earth from the Sun.

Finally an allowance was made for the angular size of the Sun by dividing the Sun's disk into zones whose distance from the point Q (Fig. 10) had the values $1{\cdot}0s$, $1{\cdot}5s$, etc. The area of each zone was multiplied by the appropriate value of $i$ and the products added to give a calculated value of $\mathcal{J}_F$. The results of the calculations are given in Table VI.

From Table VI it can be seen that the diffracted light for $\rho = 10^{-4}$ cm. is slightly blue, *i.e.* the intensity ratio $\mathcal{J}_F/I$ is somewhat greater at 4300 A. than 6300 A. On the other hand for $\rho \geqslant 10^{-2}$ cm., $\mathcal{J}_F/I$ is proportional to $\lambda$ and the diffracted light somewhat red. Light diffracted by particles of radius $10^{-3}$ cm. would have the same intensity distribution as the Sun. Neither the large nor the small particles would produce by diffraction enough colour to be readily detected by coronal observations. The observations have shown (see

Sections 6 and 8) that the colour of the Fraunhofer component is either the same as or slightly redder than that of the Sun, and hence they indicate that the radii of the diffracting particles are $10^{-3}$ cm. or greater.

TABLE VI

*Tabulated values give $\mathcal{J}_F/(I\rho N_E)$ corrected for the angular size of the Sun. Values of $\mathcal{J}_F/(I\rho N_E)$ for $\rho > 10^{-2}$ cm. are the same as for $\rho = 10^{-2}$ cm.*

| $N(r)$ | $R/s$ | $\rho = 10^{-4}$ cm. | | $\rho = 10^{-3}$ cm. | | $\rho = 10^{-2}$ cm. | |
|---|---|---|---|---|---|---|---|
| | | 4300 *A.* | 6300 *A.* | 4300 *A.* | 6300 *A.* | 4300 *A.* | 6300 *A.* |
| $N_E$ | 1·5 | $7{\cdot}7 \times 10^{7}$ | $5{\cdot}1 \times 10^{7}$ | $3{\cdot}4 \times 10^{9}$ | $3{\cdot}2 \times 10^{9}$ | $6{\cdot}0 \times 10^{9}$ | $8{\cdot}9 \times 10^{9}$ |
| | 2·0 | $5{\cdot}7 \times 10^{7}$ | $3{\cdot}9 \times 10^{7}$ | $1{\cdot}9 \times 10^{9}$ | $2{\cdot}0 \times 10^{9}$ | $2{\cdot}6 \times 10^{9}$ | $3{\cdot}8 \times 10^{9}$ |
| | 2·5 | $4{\cdot}3 \times 10^{7}$ | $3{\cdot}1 \times 10^{7}$ | $9{\cdot}5 \times 10^{8}$ | $1{\cdot}2 \times 10^{9}$ | $1{\cdot}0 \times 10^{9}$ | $1{\cdot}5 \times 10^{9}$ |
| $N_E(D/r)$ | 1·5 | $8{\cdot}4 \times 10^{8}$ | $7{\cdot}5 \times 10^{8}$ | $8{\cdot}5 \times 10^{9}$ | $8{\cdot}6 \times 10^{9}$ | $1{\cdot}3 \times 10^{10}$ | $1{\cdot}9 \times 10^{10}$ |
| | 2·0 | $5{\cdot}1 \times 10^{8}$ | $4{\cdot}7 \times 10^{8}$ | $4{\cdot}3 \times 10^{9}$ | $4{\cdot}4 \times 10^{9}$ | $5{\cdot}7 \times 10^{9}$ | $8{\cdot}1 \times 10^{9}$ |
| | 2·5 | $3{\cdot}1 \times 10^{8}$ | $2{\cdot}9 \times 10^{8}$ | $1{\cdot}9 \times 10^{9}$ | $2{\cdot}5 \times 10^{9}$ | $2{\cdot}3 \times 10^{9}$ | $3{\cdot}3 \times 10^{9}$ |
| $N_E(D/r)^2$ | 1·5 | $4{\cdot}7 \times 10^{10}$ | $4{\cdot}9 \times 10^{10}$ | $1{\cdot}3 \times 10^{11}$ | $1{\cdot}7 \times 10^{11}$ | $1{\cdot}5 \times 10^{11}$ | $2{\cdot}2 \times 10^{11}$ |
| | 2·0 | $2{\cdot}5 \times 10^{10}$ | $2{\cdot}7 \times 10^{10}$ | $6{\cdot}1 \times 10^{10}$ | $8{\cdot}0 \times 10^{10}$ | $6{\cdot}5 \times 10^{10}$ | $9{\cdot}5 \times 10^{10}$ |
| | 2·5 | $1{\cdot}2 \times 10^{10}$ | $1{\cdot}4 \times 10^{10}$ | $2{\cdot}5 \times 10^{10}$ | $3{\cdot}4 \times 10^{10}$ | $2{\cdot}6 \times 10^{10}$ | $3{\cdot}7 \times 10^{10}$ |

The rate of change of $\mathcal{J}_F$ with $R$ is not particularly sensitive to the form of $N(r)$, and the three distributions computed when applied to $\rho = 10^{-3}$ cm. are all in reasonable agreement with the observations plotted in Fig. 6. The rate of decrease of $\mathcal{J}_F$ with $R$ becomes somewhat greater for $\rho \geqslant 10^{-2}$ cm. and less for $\rho = 10^{-4}$ cm.

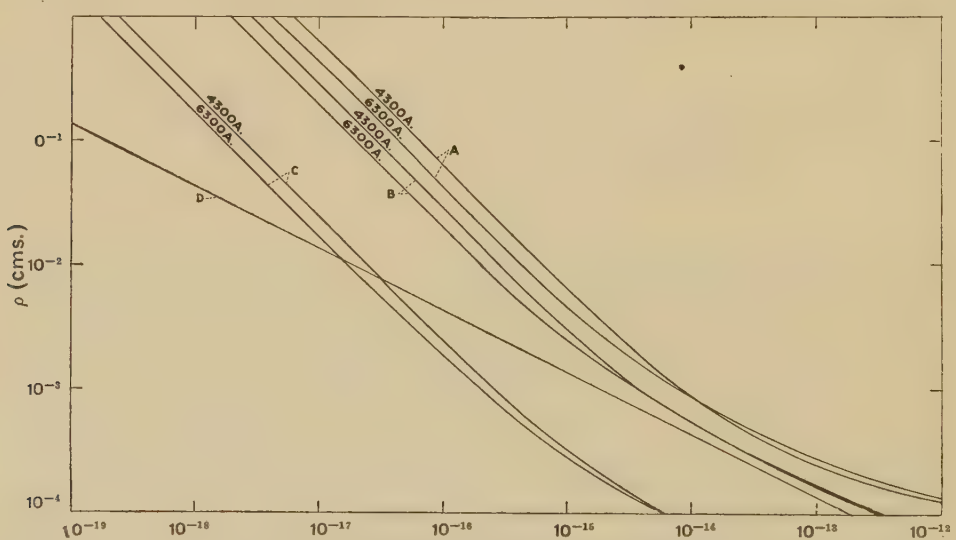


FIG. 11.—*Relation between radius of particles and number per c.c.*

A—*Corona* $N(r) = N_E$. C—*Corona* $N(r) = N_E(D/r)^2$.

B—*Corona* $N(r) = N_E(D/r)$. D—*Zodiacal light.*

In order to apply the values given in Table VI to the corona it is convenient to note from Fig. 6 that for $R = 2{\cdot}0s$ $\mathcal{J}_F/I = 1{\cdot}6 \times 10^{-8}$. Using this value one can determine $N_E$ as a function of $\rho$, and the resulting curves have been plotted in Fig. 11. The curves are given for the three distributions of particles (A), $N(r) = N_E$; (B), $N(r) = N_E(D/r)$; and (C), $N(r) = N_E(D/r)^2$. The fact that the curves for the cases A and B differ so little shows

clearly that only a small part of the light is diffracted by particles quite close to the Sun. Probably the case B is the closest approximation to reality as it agrees fairly well with Hoffmeister's empirical distribution * from $r = 0{\cdot}5\ D$ to $1{\cdot}0\ D$, and does not imply a large increase of density close to the Sun.

As the zodiacal light is also thought to be scattered from equatorial interplanetary particles, we now compute in a similar manner the intensity of light reflected from particles for which $\theta$ is large. Referring again to Fig. 10, it can be seen that the light sent per solid angle towards the Earth per c.c. at P

$$= \text{radiant flux from Sun} \times \text{scattering coefficient}$$
$$= I\pi s^2/r^2 \times N\pi\rho^2\epsilon\phi(\alpha),$$

where $\alpha = \pi - \theta$, $\phi(\alpha)$ varies from $1{\cdot}0$ at $\alpha = 0$ to $0{\cdot}0$ at $\alpha = 180°$, and $\epsilon$ is the reflection coefficient. $\epsilon$ is about $0{\cdot}7$ times the albedo and is used here in order to follow the convention $\phi(0) = 1{\cdot}0$. $\phi(\alpha)$, which is sometimes called the phase curve, has been tabulated.†

The intensity of the light received at the Earth at elongation $e$ is

$$I\pi^2 s^2\rho^2\epsilon\int_0^\infty \frac{1}{r^2}N(r)\phi(\alpha)dL$$
$$= \mathcal{J}.I\pi^2 s^2\rho^2\epsilon N_E/D,$$

where

$$\mathcal{J} = \operatorname{cosec} e\int_{\alpha_0}^{\pi - e} f(r)\phi(\alpha)d\alpha.$$

$N_E$ is the value of $N(r)$ at the distance of the Earth, and $N(r) = N_E f(r)$. The curve $\mathcal{J}$ as a function of $e$ has been studied both theoretically and empirically by Hoffmeister † and for $e = 40°$ $\mathcal{J}$ has the value $1{\cdot}0$.

The intensity of the zodiacal light at $e = 40°$ is found ‡ to be 800 tenth magnitude stars per square degree, which is $6 \times 10^{-13}$ times the intensity of the Sun's surface.

Thus

$$\pi^2 s^2\rho^2\epsilon N_E = 6 \times 10^{-13}D,$$

and inserting

$$s = 7 \times 10^{10} \text{ cm.}, \qquad \epsilon = 0{\cdot}1, \qquad D = 1{\cdot}5 \times 10^{13} \text{ cm.},$$

gives

$$\rho^2 N_E = 1{\cdot}8 \times 10^{-21} \text{ cm.}^{-1}.$$

This relation between $\rho$ and $N_E$ is also given in Fig. 11. It should be possible in principle to determine both $\rho$ and $N_E$ from the intersection of the coronal and zodiacal light curves in this diagram. Restricting our attention to the most plausible case $N(r) = N_E(D/r)$ we notice that this coronal curve does not quite intersect the zodiacal light curve. However, there are several factors not accurately determined, for example $\epsilon$ has arbitrarily been given the value $0{\cdot}1$, representing an albedo of $0{\cdot}14$. A total error of a factor of 2 might be expected, and, if this is allowed, agreement between the corona and the zodiacal light is reached for $\rho \leqslant 10^{-3}$ cm. A reasonable solution is

$$\rho = 10^{-3} \text{ cm.} \quad \text{and} \quad N_E = 3 \times 10^{-15} \text{ cm.}^{-3}.$$

We conclude that if the zodiacal light is scattered by particles of radius $10^{-3}$ cm. or less the particles would produce a Fraunhofer component $\mathcal{J}_F$ of the corona with an intensity, and an intensity distribution with $R$ and $\lambda$, almost the same as that actually observed.

* C. Hoffmeister, *Veröff. Sternw. Babelsberg*, 10, 12–19, 1932; *Handb. Astrophys.*, II/1, 157–162, 1929.

† Hoffmeister, *loc. cit.*

‡ C. J. Elvey and F. E. Roach, *Ap. J.*, 85, 213, 1937.

The red shift of the coronal Fraunhofer lines is still a difficulty, as it was in Grotrian's original theory. It might be possible to account for the particles having radial velocities of the order required (20 km./sec.), but this would not appreciably affect the wave-length of light diffracted at small angles.

*Acknowledgments.*—The author wishes to acknowledge generous help received in South Africa. Arrangements for the eclipse camp were in the hands of Dr. Jackson of the Royal Observatory, Cape of Good Hope, and much assistance was received from Dr. Redman of the Radcliffe Observatory during the month preceding the eclipse. The camp itself was in the private grounds of Mr. Fred Laurence of Calvinia, and Mr. and Mrs. Laurence were most generous with their hospitality. Assistance in making the actual exposures was given by Mr. Gilmore and Mr. Menzies of the University of Cape Town, and the mirrors were silvered by Dr. Paraskevopoulos of the Boyden Station, Bloemfontein. Finally the author was privileged to use the excellent microphotometer of the Radcliffe Observatory for examining the eclipse spectrograms.

Cœlostats were lent by the Sydney Observatory and Physics Department of the Sydney University. Wave-lengths of the coronal absorption lines were measured by Mr. Chamberlain and Dr. Gascoigne of the Commonwealth Observatory staff. The observing programme was planned by the Commonwealth Astronomer, Dr. Woolley, who was unable to accompany the expedition but has been closely associated with the work.

*Commonwealth Observatory,*
*Mount Stromlo,*
*Canberra:*
1945 *December.*

# PHOTOVISUAL MAGNITUDES OF SOUTHERN STARS

*A. W. J. Cousins*

(Received 1945 December 29)

*Summary*

A second series of photovisual observations of bright stars using the Fabry method was secured in 1944. The magnitudes of 67 stars have been determined with a probable error not exceeding $\pm 0^m.05$.

---

1. *Introduction.*—Photovisual magnitudes of a number of naked eye and some fainter stars were obtained in 1942 *, using the Fabry method. The colour system adopted as standard was that of the Kodak Super XX film and Wratten 11 colour filter. The observations were discontinued because of war restrictions, but in 1944 it was possible to resume them using pre-war Agfa Isochrom film. As this film proved considerably slower than those previously used, the programme was restricted to the brighter stars. The magnitudes of 67 stars, most of them brighter than $4^m.0$, were obtained.

2. *Method of Observation.*—Apart from minor changes, the same equipment and method of observation were employed as for the first series, but only the Wratten 11 colour filter was used. Arrangements for adjusting the sensitometer lamp obviated the need for a time correction, but an attempt to use a colour filter when calibrating the films met with difficulties. As no sensible difference in scale could be detected, it was decided to work without a filter as previously.

Using figures supplied by the makers for the transmission of the filter, and data on the sensitivity of the Agfa Isochrom plate given in *Annales d'Astrophysique*, $2^e$ Ann., 369, 1939, it appears that the effective wave-length is near 5160 A. The colour equation compared with the first series was found to be +0.15 C.I. This implies an effective wave-length of 5350 A. for the first series, in general agreement with the second value given in the earlier paper.

The films were developed by running them in and out of the developer, a practice that is believed to be responsible for a certain amount of background fog. Asymmetrical effects, of the type recently studied by D. R. Barber †, are also evident and this practice will be discontinued in future work.

3. *Measurement and Reduction.*—All the images were measured photo-electrically using a Photronic cell and galvanometer. Measures of the calibration strips showed considerable lack of uniformity, so these were combined to give mean characteristics for each film. This unevenness is attributed to the age of the films and the fact that roll film is always in contact and subject to a certain amount of pressure on the emulsion side. Where the pressure had been especially heavy the fogging was pronounced.

The zero point of the present series was established by including a number of stars from the "Main Programme" (Table II) of the first series and reducing their magnitudes to the present system by means of the colour coefficient.

Corrections for atmospheric extinction were applied as previously, making use of stars at low altitudes as a guide.

4. *Results.*—The individual observations are of considerably lower precision than those of the first series, the average mean error being about $\pm 0^m.08$. This was to be expected when using old films. In order to improve the accuracy of the resulting

* *M.N.*, **103**, 154, 1943. Referred to as first series.

† *M.N.*, **104**, 335, 1944.

magnitudes, it was decided to include the earlier observations of the "Bright Stars" given in Table III of the previous paper.* The old films were remeasured, and the results combined with those of the present series using appropriate colour corrections. The individual observations were weighted according to the residuals for each night, and combined to give the magnitudes in the third column of the table. The probable error based on the internal agreement of the observations is generally less than $0^m.025$. Inferior results are marked with a colon. When the probable error exceeded $0^m.05$ the star was omitted.

*Photovisual Magnitudes of Southern Stars*

| Star | Spect. | Magnitude | | Star | Spect. | Magnitude | |
|---|---|---|---|---|---|---|---|
| | | *Pv* (2) | *Pv* (1) | | | *Pv* (2) | *Pv* (1) |
| σ Pupp | K5 | 3·55 | 3·33 | γ Musc | B5 | 3·90 | 3·95 |
| ξ Pupp | Gop | 3·61 | 3·52 | β Corv | G5 | 2·85: | 2·73 |
| a Pupp | G5 | 3·99 | 3·87 | α Musc | B5 | 2·68 | 2·73 |
| χ Cari | B3 | 3·52 | 3·57 | γ Cent | Ao | 2·22 | 2·24 |
| ρ Pupp | F5 | 2·96 | 2·92 | β Musc | B3 | 3·07 | 3·12 |
| γ Velr | OW+B3 | 1·64: | 1·70 | β Cruc | B1 | 1·22 | 1·28 |
| ε Cari | Ko+B | 2·10 | 1·94 | δ Musc | K2 | 3·96 | 3·77 |
| β Pyxi | G5 | 4·28 | 4·16 | γ Hyda | G5 | 3·26: | 3·14 |
| o Velr | B3 | 3·66 | 3·71 | ι Cent | A2 | 2·81: | 2·82 |
| α Pyxi | B2 | 3·77 | 3·83 | ε Cent | B2 | 2·30 | 2·36 |
| δ Velr | Ao | 1·90: | 1·92 | ν Cent | B2 | 3·43: | 3·48 |
| γ Pyxi | K2 | 4·38 | 4·19 | μ Cent | B3 | 3·26: | 3·30 |
| c Cari | B8 | 3·88 | 3·92 | ζ Cent | B3 | 2·51: | 2·56 |
| λ Velr | K5 | 2·59 | 2·37 | β Cent | B1 | 0·52 | 0·57 |
| a Cari | B3 | 3·48 | 3·53 | θ Cent | Ko | 2·29 | 2·13 |
| β Cari | Ao | 1·65 | 1·67 | α Boot | Ko | 0·14 | −0·02 |
| ι Cari | Fo | 2·30 | 2·28 | η Cent | B3 | 2·35 | 2·39 |
| κ Velr | B3 | 2·45 | 2·50 | α Cent | Go+K5 | −0·27 | −0·36 |
| N Velr | K5 | 3·49 | 3·27 | α Circ | Fo | 3·23: | 3·21 |
| v Cari | Fo | 3·04 | 3·02 | α Lupi | B2 | 2·33 | 2·37 |
| φ Velr | B5 | 3·54 | 3·59 | β Libr | B8 | 2·70: | 2·74 |
| ω Cari | B8 | 3·36 | 3·40 | α Trau | K2 | 2·19 | 2·00 |
| q Velr | K5 | 3·70 | 3·48 | ε Scor | Ko | 2·50: | 2·34 |
| p Cari | B5p | 3·33 | 3·38 | α Arae | B3p | 2·90: | 2·95 |
| θ Cari | Bo | 2·73 | 2·78 | λ Scor | B2 | 1·54 | 1·60 |
| μ Velr | G5 | 2·91 | 2·79 | θ Scor | Fo | 1·92 | 1·90 |
| v Hyda | Ko | 3·40 | 3·24 | κ Scor | B2 | 2·35: | 2·41 |
| u Cari | Ko | 3·99: | 3·83 | ε Sgtr | Ao | 1·83 | 1·85 |
| λ Cent | B9 | 3·16 | 3·19 | σ Sgtr | B3 | 2·08 | 2·11 |
| δ Cent | B3 | 2·70 | 2·75 | ζ Sgtr | A2 | 2·66 | 2·67 |
| δ Cruc | B3 | 2·77 | 2·83 | α Pavo | B3 | 1·96 | 2·00 |
| γ Corv | B8 | 2·54: | 2·58 | α Grus | B5 | 1·53 | 1·58 |
| α Cruc | B1+B1 | 0·66 | 0·72 | β Grus | Mb | 2·34: | 2·09 |
| γ Cruc | Mb | 2·04 | 1·79 | | | | |

* *M.N.*, **103**, 157, 1943. These magnitudes were of lower weight than those given in Table II, and there was some uncertainty regarding the zero point. For two stars, δ Velorum and α Scorpii, the results are discordant. The magnitude now given for the former is based on the present series only. The latter star has been omitted.

The fourth column of the table gives the magnitudes reduced to the colour system and zero point of the first series. There is no detectable difference in scale, and the average deviation of 14 stars common to both series (but excluding the bright stars incorporated with the present series) is $0^m.024$. The two series can, therefore, be considered mutually consistent.

A comparison with E. G. Williams's photovisual magnitudes of early B-type stars * confirms the difference of scale found from the first series, viz. 0·04, but there is a slight difference in zero point, possibly due to a variation with R.A. in one of the series. The average deviation of 23 stars common to the two lists is $0^m.040$ without removing the difference in zero point and $0^m.034$ after doing so. These are appreciably larger than the value found from the first series.

Adopting the effective wave-lengths for the international photographic and photovisual magnitudes derived by Seares and Joyner †, the colour equation of the first series relative to the international photovisual system should be about +0·16 C.I.

*Acknowledgment.*—The writer is especially indebted to Dr. Zanstra for facilities for measuring the films in the Department of Physics at Howard College, Durban.

*Durban:*
1945 *November.*

* *M.N.*, 102, 231, 1942.
† *Contr. Mt. Wilson Obs.*, No. 685; *Ap. J.*, 98, 302, 1943.

# DOUBLE STAR MEASURES—SECOND SERIES

*W. P. Hirst*

(Communicated by H.M. Astronomer)

(Received 1946 February 5*)

The following measures were made with the 7-inch refractor at the Royal Observatory at the Cape by kind permission of H.M. Astronomer, Dr. J. Jackson.

The columns from left to right give: Name and ADS number if any; right ascension and southern declination (equinox 1900·0); date (omitting century); hour angle; position angle; position angle with reversing prism minus angle without prism; distance; magnitude difference (estimated); remarks.

| Name | Position | Date 1900 + | Hour angle | Position angle | | Distance | Δ Mag. | |
|---|---|---|---|---|---|---|---|---|
| | h m | | h | ° | ° | ″ | | |
| I 260 | 0 27·0 | 43·795 | −3·7 | 293·0 | +4·4 | 0·4 (est.) | 0·4 | 2 n |
| $\beta_2$ Tucn | 63° 31′ | 44·745 | −3·3 | 297·5 | −1·2 | 0·45 (est.) | 1·0 | 1 n |
| Slr I | 1 01·6 | 43·994 | +2·4 | 351·6 | −0·8 | 1·29 | 0 | 1 n |
| | 47° 15′ | | | | | | | ρ low |
| Jc. 8 A–B | 3 08·9 | 44·140 | +3·2 | 185·7 | +1·2 | 0·75 | 0·3 | 2 n † |
| | 44° 48′ | | | | | | | |
| h 3556 A–C | 3 08·9 | 44·134 | +3·0 | 201·9 | +1·2 | 3·47 | 4·0 | 1 n |
| | 44° 48′ | | | | | | | |
| Δ 16 | 3 44·9 | 43·244 | +4·2 | 210·4 | +1·0 | 7·64 | ... | 1 n |
| f Erid. | 37° 56′ | 44·144 | +3·0 | 211·4 | +1·1 | 7·73 | 0·4 | 2, 1 n |
| β 1004 | 3 58·2 | 43·244 | +3·5 | 115·2 | +0·9 | 1·50 | 0·5 | 1 n |
| | 34° 46′ | 44·140 | +2·7 | 116·4 | −1·5 | 1·67 | 0·3 | 2 n |
| Gale I | 4 14·8 | 43·244 | +4·0 | 34·0 | ... | 0·7 (est.) | ... | 1 n |
| | 61° 12′ | 44·331 | +5·7 | 19·7 | −7·3 | 0·7 (est.) | 0·3 | 1 n |
| β 744 | 4 17·4 | 43·244 | +4·1 | 248·4 | −1·0 | 0·8 (est.) | ... | 1 n |
| ADS 3159 | 25° 58′ | | | | | | | |
| β 184 | 4 23·6 | 43·200 | +4·0 | 253·9 | ... | 1·52 | 1·5 | 3 n |
| | 21° 44′ | | | | | | | |
| β 746 | 4 27·9 | 43·244 | +4·4 | 7·7 | ... | 1·17 | ... | 1 n |
| | 36° 07′ | | | | | | | |
| h 3683 | 4 38·6 | 43·224 | +3·7 | 93·0 | −0·6 | 1·47 | 0·0 | 3 n |
| | 59° 08′ | | | | | | | |
| I 342 | 4 47·4 | 43·244 | +4·4 | 152·1 | −0·3 | 1·64 | ... | 1 n |
| | 54° 04′ | | | | | | | |
| h 3752 | 5 17·7 | 43·227 | +3·7 | 98·8 | +1·9 | 2·90 | ... | 2 n |
| | 24° 52′ | 44·323 | +4·7 | 98·3 | +0·3 | 3·08 | 1·6 | 2 n |
| I 276 | 5 27·5 | 43·227 | +3·8 | 176·3 | −1·7 | 0·87 | ... | 2 n |
| | 68° 42′ | 44·323 | +4·8 | 177·7 | −1·9 | 1·08 | 0·0 | 3 n |

* Originally submitted in different form on 1943 May 3.

† ρ too large.

| Name | Position | Date 1900+ | Hour angle | Position angle | | Distance | Δ Mag. | |
|---|---|---|---|---|---|---|---|---|
| | h m | | h | ° | ° | ″ | | |
| h 3823 | 5 56·6 | 44·323 | +4·3 | 77·7 | +0·2 | 2·00 | 0·1 | 3 n |
| | 31° 03′ | | | | | | | |
| Δ 23 | 6 02·2 | 43·325 | +4·0 | 85·0 | +1·2 | 1·78 | 0·5 | 2, 1 n |
| | 48° 27′ | 44·318 | +4·6 | 86·1 | +1·8 | 1·91 | 0·3 | 4 n |
| β 754 | 6 31·1 | 44·323 | +4·5 | 47·3 | −2·0 | 0·88 | 0·3 | 2 n |
| | 33° 56′ | | | | | | | |
| I 312 | 7 18·7 | 44·331 | +4·1 | 161·7 | −3·7 | 1·36 | 0·1 | 1 n |
| | 75° 41′ | | | | | | | |
| Δ 52 | 7 30·1 | 44·330 | +4·0 | 113·3 | −0·4 | 9·36 | 0·0 | 3 n |
| | 23° 15′ | | | | | | | |
| Σ 1157 | 7 50 | 43·110 | −1·3 | 228·9 | ... | 0·98 | 0·0 | 1 n |
| | 2° 32′ | | | | | | | |
| I 26 | 7 54·4 | 44·331 | +4·5 | 53·8 | +1·9 | 1·08 | 0·6 | 1 n |
| | 47° 37′ | | | | | | | |
| I 489 | 8 27·0 | 44·315 | +3·4 | 85·6 | +4·7 | 0·5 (est.) | 0·5 | 1 n |
| | 19° 14′ | | | | | | | |
| β 208 | 8 34·8 | 43·325 | +2·3 | 208·9 | +0·3 | 1·82 | 1·2 | 2, 1 n |
| ADS 6914 | 22° 19′ | 44·323 | +3·5 | 211·4 | −0·3 | 1·95 | 1·3 | 2 n |
| h 4220 | 9 30·2 | 43·192 | −1·8 | 111·4 | ... | 1·88 | ... | 1 n |
| | 48° 34′ | | | | | | | |
| Rümker 11 | 9 44·6 | 43·192 | −2·4 | 126·2 | ... | 4·59 | 3·0 | 1 n |
| | 64° 36′ | | | | | | | |
| I 292 | 9 59·3 | 43·192 | −2·0 | 166·8 | ... | 0·5 (est.) | ... | 1 n |
| | 27° 54′ | | | | | | | |
| γ Leon | 10 14·5 | 43·353 | +0·8 | 120·5 | −2·1 | 4·17 | 0·5 | 1 n |
| ADS 7724 | 20° 21′ | | | | | | | |
| h 4478 | 11 47·9 | 43·211 | −2·6 | 0·6 | ... | 1·17 | ... | 1 n |
| | 33° 21′ | | | | | | | |
| α Cruc | 12 21·0 | 43·192 | −5·3 | 113·8 | ... | 4·73 | 0·0 | 1 n |
| | 62° 33′ | | | | | | | |
| γ Cent | 12 36 | 43·360 | −1·1 | 13·1 | −2·0 | 0·93 | 0·0 | 3 n |
| | 48° 25′ | 44·301 | −1·9 | 11·7 | −4·4 | 0·87 | 0·0 | 1 n |
| R 207 | 12 40·2 | 45·509 | +3·4 | 6·8 | −0·6 | 1·55 | 0·0 | 1 n |
| | 67° 33′ | | | | | | | |
| α Cent | 14 32·8 | 43·338 | −4·1 | 2·8 | −0·8 | 7·87 | 1·8 | 4 n |
| | 60° 25′ | | | | | | | |
| h 4728 | 14 58·3 | 43·638 | +3·0 | 76·0 | −0·7 | 1·70 | 0·0 | 3 n |
| Π Lupi | 46° 40′ | | | | | | | |
| h 4753 | 15 11·6 | 43·764 | +4·8 | 145·7 | −0·2 | 1·38 | 0·3 | 2 n |
| | 47° 30′ | | | | | | | |

| Name | Position | Date 1900 + | Hour angle | Position angle | | Distance | Δ Mag. | |
|---|---|---|---|---|---|---|---|---|
| | h m | | h | ° | ° | ″ | | |
| h 4757 | 15 15·4 | 43·783 | +5·7 | 58·6 | +0·4 | 1·07 | 0·2 | 2 n |
| | 58° 58′ | 44·745 | +5·3 | 51·2 | −0·6 | 1·26 | 0·0 | 1 n |
| λ 258 A–B | 15 55·4 | 43·788 | +5·5 | 283·8 | +2·5 | 0·35 (est.) | 0·4 | 3, 2 n |
| | 57° 30′ | 44·745 | +4·4 | 271·5 | +0·6 | 0·35 (est.) | 0·7 | 1 n |
| h 4825 (λ 258 AB–C) | 15 55·4 57° 30′ | 43·772 | +5·4 | 245·8 | +0·3 | 10·61 | 3·5 | 1 n |
| ℍ II 19 | 16 19·6 23° 13′ | 43·555 | 0·0 | 347·0 | −0·7 | 3·52 | 0·5 | 3, 1 n |
| Melb. 4 A–B | 17 12·8 | 43·631 | +0·5 | 292·3 | +1·1 | 2·15 | 1·3 | 6 n |
| | 34° 53′ | 44·454 | −1·6 | 289·6 | +0·7 | 2·05 | 1·2 | 3 n |
| h 4949 | 17 19·5 45° 45′ | 43·657 | +1·7 | 256·8 | +0·8 | 2·45 | 0·3 | 3, 1 n |
| h 5014 | 17 59·6 43° 26′ | 43·772 | +3·3 | 215·2 | −0·6 | 1·84 | 0·0 | 3 n |
| Hd 150 | 18 56·2 30° 01′ | 43·700 | +1·1 | 69·5 | −0·6 | 0·4 (est.) | 0·2 | 3 n |
| h 5084 | 18 59·7 37° 12′ | 43·814 | +3·4 | 53·8 | +0·7 | 2·66 | 0·0 | 3 n |
| I 119 | 19 34·0 59° 14′ | 43·822 | +3·3 | 162·6 | +3·4 | 1·54 | 1·3 | 2 n |
| β 763 | 20 17·1 42° 45′ | 43·859 | +3·2 | 228·7 | −0·1 | 1·15 | 1·0 | 3, 2 n |
| Rümker 26 | 20 43·3 62° 48′ | 43·902 | +3·8 | 88·6 | +0·8 | 2·39 | 0·2 | 3 n |
| h 5246 | 21 03·1 54° 59′ | 43·891 | +3·5 | 128·2 | −0·4 | 3·65 | 0·1 | 2 n |
| h 5258 | 21 12·7 53° 52′ | 43·902 | +3·6 | 276·1 | +0·1 | 5·26 | 2·3 | 3 n |

*Cape Town:*
1945 *December* 31.